SKB

TECHNICAL REPORT 96-11

Thermoelastic stress due to an instantaneous finite line heat source in an infinite medium

Johan Claesson, Göran Hellström

Depts. of Building Physics and Mathematical Physics,
Lund University, Lund, Sweden

September 1995

SVENSK KÄRNBRÄNSLEHANTERING AB
SWEDISH NUCLEAR FUEL AND WASTE MANAGEMENT CO
P.O.BOX 5864 S-102 40 STOCKHOLM SWEDEN
PHONE +46 8 665 28 00
FAX +46 8 661 57 19

THERMOELASTIC STRESS DUE TO AN INSTANTANEOUS FINITE LINE HEAT SOURCE IN AN INFINITE MEDIUM

Johan Claesson, Göran Hellström

Depts. of Building Physics and Mathematical Physics, Lund University, Lund, Sweden

September 1995

THERMOELASTIC STRESS DUE TO AN INSTANTANEOUS FINITE LINE HEAT SOURCE IN AN INFINITE MEDIUM

JOHAN CLAESSON
GÖRAN HELLSTRÖM

September 1995

Depts. of Building Physics and Mathematical Physics
Lund University, Sweden

Keywords: Thermoelastic stress, finite line heat source, antisymmetric infinite source, three-dimensional time-dependent analytical solution.

Contents

	Abstract/Sammanfattning	1
1	Introduction	2
2	Mathematical problem	3
3	Thermoelastic equations	4
4	Temperature in the antisymmetric case	5
5	Dimensionless formulation	6
6	Displacement potential Φ_a	8
7	Displacement field	9
8	Strain field	10
9	Stress field	11
10	Principal stresses	13
11	Asymptotic behavior	14
12	Development with time	16
13	Finite line source	16
14	Time-dependent heat source	17
15	Summary of main formulas	18
	References	18
	Nomenclature	19
	Figures 3-16	20
	Appendix 1. Behavior for large radius	29
	Appendix 2. Behavior for small radius	30

Abstract

The thermoelastic response due to a line heat source of finite length in an infinite medium is analyzed. The problem originates from studies of nuclear waste repositories in rock. The idea is to deposit canisters containing nuclear waste along boreholes very deep below the ground surface. An important concern is that dangerous waste from damaged canisters may eventually reach the biosphere by groundwater moving in cracks and fractures in the rock. The stress and strain fields are therefore of main interest, since they influence crack formation and crack widths.

The problem is by superposition reduced to the case of a single, infinite, antisymmetric, instantaneous line heat source. The dimensionless problem turns out to depend on the dimensionless radial and axial coordinates only, although the original time-dependent problem contains several parameters.

An exact analytical solution is derived. The solution is surprisingly handy, considering the complexity of the initial problem. The radial and axial displacements u and w become:

$$u = \frac{\Phi_0}{\rho}\left[\frac{z}{r}\operatorname{erf}\left(\frac{r}{\sqrt{4at}}\right) - e^{-\rho^2/(4at)}\operatorname{erf}\left(\frac{z}{\sqrt{4at}}\right)\right] \qquad w = -\frac{\Phi_0}{r}\operatorname{erf}\left(\frac{r}{\sqrt{4at}}\right)$$

The stress and strain fields are readily obtained from derivatives of the displacement components. These fields are studied and presented in detail. Asymptotic behavior, field of principal stresses, regions of compression and tension, and largest values of compression and tension of the components are given from exact formulas.

The solution may be used to test numerical models for coupled thermoelastic processes. It may also be used in more detailed numerical simulations of the process near the heat sources as boundary conditions to account for the three-dimensional global process.

Sammanfattning

Den termoelastiska responsen för en ändlig linjekälla i en oändlig omgivning analyseras. Problemet härrör från studier av kärnbränslelager i berg. Konceptet innebär att kapslar med kärnbränsle placeras i borrhål mycket djupt ner under markytan. Farligt avfall från skadade kapslar kan potentiellt nå biosfären med grundvatten som strömmar i sprickor i berget. Töjnings- och spänningsfälten är därför av intresse eftersom dessa påverkar spickbildning och sprickvidd.

Problemet reduceras genom superposition till fallet med en enskild, oändlig, antisymmetrisk, momentan linjekälla. Det dimensionslösa problemet visar sig bero enbart på de dimensionslösa radiella och axiella koordinaterna, trots att det ursprungliga problemet innehåller åtskilliga parametrar.

En exakt analytisk lösning härleds. Lösningen är förvånansvärt hanterlig, om man beaktar det ursprungliga problemets komplexitet. De radiella och axiella förskjutningarna u och w blir:

$$u = \frac{\Phi_0}{\rho}\left[\frac{z}{r}\operatorname{erf}\left(\frac{r}{\sqrt{4at}}\right) - e^{-\rho^2/(4at)}\operatorname{erf}\left(\frac{z}{\sqrt{4at}}\right)\right] \qquad w = -\frac{\Phi_0}{r}\operatorname{erf}\left(\frac{r}{\sqrt{4at}}\right)$$

Spännings- och töjningsfälten erhålls från derivator av förskjutningskomponenterna. Dessa fält studeras och presenteras i detalj. Asymptotiska beteenden, huvudspänningsfält, områden med kompression och dragspänning samt maximivärden för tryck- och dragspänning anges av exakta formler.

Lösningen kan användas för att testa numeriska modeller för kopplade termoelastiska processer. Den kan också utnyttjas i mer detaljerade numeriska simuleringar av förloppet nära värmekällorna som randvillkor för att få med den mer globala tredimensionella processen.

1 Introduction

Figure 1A shows one of the concepts for final storage of nuclear waste studied by The Swedish Nuclear and Waste Management Co (SKB. Annual and technical reports, 1980-94). The canisters containing the nuclear waste are to be placed along deep boreholes in hard rock from 2 000 m to 4 000 m depth. Other possibilities are to use boreholes drilled from tunnels deep below the ground surface.

The capsules release heat due to radioactive decay. The nuclear waste repository creates a number of line heat sources in the rock mass. The released heat warms the rock and induces a thermoelastic stress field.

The rock mass serves as a protective barrier. In the worst-case scenario, groundwater may transport nuclear waste all the way from damaged canisters to the biosphere. Groundwater flow requires an open fracture and crack system. The stress and strain fields are therefore of main interest, since they influence crack closure, opening, formation and widths.

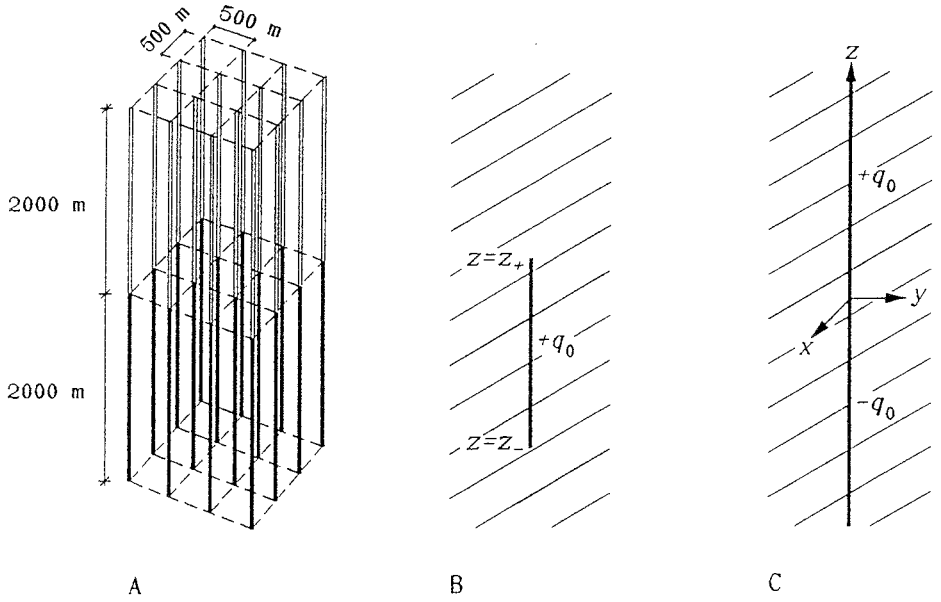

Figure 1: A: Nuclear waste repository using deep boreholes. B: Finite line heat source due to one of the boreholes. C: Instantaneous, infinite, antisymmetric line heat source in an infinite elastic medium.

The purpose of this study is to analyze the thermoelastic process in the rock caused by these line heat sources. The process is of interest for very long time-scales. The behavior in and around the repository region, but also far away from the canisters, is of interest.

An exact analytical solution for the time-dependent, three-dimensional process is derived. The solution, which is not valid in the immediate vicinity of single canisters with their local complications, is surprisingly simple.

General references for thermoelasticity is Boley and Weiner (1960) and Parkus (1959). General formulas used here are taken from the latter reference. The two-dimensional problem for an infinite line heat source may be found in textbooks, for example Timoshenko and Goodier (1970). In our literature search, we did not find any solution for the finite line heat source or the antisymmetric infinite source.

2 Mathematical problem

The linearly elastic, isotropic, homogeneous medium has infinite extensions in all directions. The effect of the ground surface boundary 2 000 m above the top of the line sources is *neglected.* The thermoelastic strain and stress fields are caused by the temperature field $T(x, y, z, t)$ of an instantaneous line heat source that lies along the z-axis. The basic case considered here is what will be called an *infinite, antisymmetric* line heat source. At $t = 0$, the heat $+q_0$ (J/m) is released along the positive z-axis ($0 < z < \infty$) and the heat $-q_0$ along the negative axis ($0 > z > -\infty$). See Fig. 1:C.

The case of a finite line heat source, Fig. 1:B, is obtained by superposition of two antisymmetric sources. See Section 13 and in particular Eqs. (92-94). This case is not dealt with in any detail in this paper. The heat release from the nuclear waste is actually a decreasing function of time: $q_0 = q_0(t)$. Here, the basic case of instantaneous heat release at $t = 0$ is studied. The thermoelastic solution for any $q_0(t)$ is readily obtained by Duhamel's superposition theorem (Carslaw and Jaeger 1959). The basic formulas are given in Section 14, but this further step in the analysis is not dealt with here.

The finite heat source with the length H introduces an additional variable. The considered antisymmetric heat source is the three-dimensional case with the highest degree of intrinsic simplicity. It provides the simplest possible solution from which the case of any set of finite line sources with time-dependent heat release is solved by superposition. An important result will be that the solution in dimensionless form does not contain *any parameters.* It becomes a function of the two dimensionless coordinates only.

The temperature field of the line heat source $T(x, y, z, t)$, considered at any particular time $t > 0$, induces a displacement field $\mathbf{u}$, a strain field ε and a stress field σ, which are to be determined (tensors are written in a larger size). The boundary condition for any heat source of finite length is that all these fields vanish at infinity, $r = \sqrt{x^2 + y^2 + z^2} \to \infty$. In the case of an infinite line heat source, this condition must be relaxed, since there is a thermal influence near the z-axis ($\rho = \sqrt{x^2 + y^2}$ finite) for $z \to \pm\infty$. This is discussed below. The displacement field $\mathbf{u}$ satisfies the vector equation (Parkus 1959, Boley and Weiner 1960):

$$\nabla^2(\mathbf{u}) + \frac{1}{1-2\nu}\nabla(\nabla \cdot \mathbf{u}) = \frac{2\alpha(1+\nu)}{1-2\nu}\nabla T \tag{1}$$

Here, α (1/K) denotes the coefficient of linear thermal expansion. The temperature field is, for any $t > 0$, regular everywhere. It tends to zero far away from the z-axis ($\rho \to \infty$).

A few thermoelastic problems may be solved by use of a single displacement potential $\Phi(x, y, z; t)$ (Parkus 1959):

$$\mathbf{u} = \nabla\Phi \tag{2}$$

Equation (1) is satisfied if Φ is a solution of

$$\nabla^2\Phi = \frac{1+\nu}{1-\nu}\alpha T \tag{3}$$

The temperature field is considered at any time $t > 0$, so $\Phi(x, y, z; t)$ depends on the spacial coordinates with t as a parameter.

Boundary conditions for the solution $\Phi(x, y, z; t)$ to Eq. (3) need to be specified. The problem is antisymmetric with respect to z, since T is an odd function of z. It turns out

to be sufficient to require that the solution Φ is an *odd* function of z and that $\nabla\Phi$ is finite at infinity. This means that Φ becomes zero for $z = 0$. We choose the condition:

$$\Phi(x, y, 0; t) = 0 \tag{4}$$

The mathematical problem is defined by Eqs. (3) and (4). The displacement is obtained by first derivatives of Φ, Eq. (2), while the strain and stress fields are given by second derivatives, Eqs. (6) and (9). The solution for the finite line heat source is obtained by superposition of two antisymmetric solutions. It will directly follow from the asymptotic expressions that the displacements indeed tend to zero at infinity for the finite heat source.

We will use cylindrical coordinates (ρ, φ, z) and, occasionally, spherical coordinates (r, φ, θ). See Fig. 2.

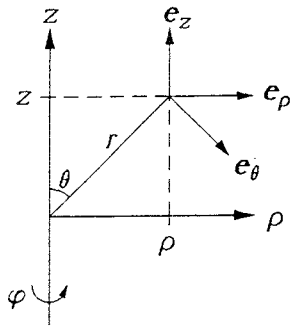

$$r = \sqrt{\rho^2 + z^2}$$
$$\rho = \sqrt{x^2 + y^2}$$
$$\sin(\theta) = \rho/r$$
$$\cos(\theta) = z/r$$

Figure 2: Cylindrical coordinates ρ, φ, z and spherical coordinates r, φ, θ.

3 Thermoelastic equations

The temperature from the line source is rotationally symmetric with respect to the z-axis. It is a function of the cylindrical coordinates ρ and z but independent of the angle φ: $T = T(\rho, z; t)$. The displacement potential, which is the solution of Eq. (3), is also independent of φ: $\Phi = \Phi(\rho, z; t)$. The displacement $\mathbf{u}$ has a *radial* component u and an axial one w:

$$\mathbf{u} = u\,\mathbf{e}_\rho + w\,\mathbf{e}_z$$
$$u(\rho, z; t) = \frac{\partial \Phi}{\partial \rho} \qquad w(\rho, z; t) = \frac{\partial \Phi}{\partial z} \tag{5}$$

The strain field ε expressed in cylindrical coordinates becomes, (Parkus 1959):

$$\varepsilon_{\rho\rho} = \frac{\partial^2 \Phi}{\partial \rho^2} \qquad \varepsilon_{\varphi\varphi} = \frac{1}{\rho}\frac{\partial \Phi}{\partial \rho}$$
$$\varepsilon_{zz} = \frac{\partial^2 \Phi}{\partial z^2} \qquad \varepsilon_{\rho z} = \frac{\partial^2 \Phi}{\partial \rho \partial z}$$
$$\varepsilon_{\rho\varphi} = 0 \qquad \varepsilon_{z\varphi} = 0 \tag{6}$$

The volume expansion e is given by:

$$e = \nabla \cdot \mathbf{u} = \nabla^2 \Phi = \frac{\partial^2 \Phi}{\partial \rho^2} + \frac{1}{\rho}\frac{\partial \Phi}{\partial \rho} + \frac{\partial^2 \Phi}{\partial z^2} = \varepsilon_{\rho\rho} + \varepsilon_{\varphi\varphi} + \varepsilon_{zz} \tag{7}$$

The stress field σ is related to the strain field by Hook's law. The thermal expansion is allowed for by subtracting αT from the diagonal strain components and replacing e by $e - 3\alpha T$. Both e and αT, Eqs. (7) and (3), are proportional to $\nabla^2\Phi$, and we get, Parkus (1959):

$$\sigma = \frac{E}{1+\nu}\left(\varepsilon - \nabla^2\Phi\, 1\right) \tag{8}$$

Here, 1 is the unit tensor. The components of the stress tensor become:

$$\begin{aligned}
\sigma_{\rho\rho} &= \frac{E}{1+\nu}\left(\frac{\partial^2\Phi}{\partial\rho^2} - \nabla^2\Phi\right) & \sigma_{\varphi\varphi} &= \frac{E}{1+\nu}\left(\frac{1}{\rho}\frac{\partial\Phi}{\partial\rho} - \nabla^2\Phi\right) \\
\sigma_{zz} &= \frac{E}{1+\nu}\left(\frac{\partial^2\Phi}{\partial z^2} - \nabla^2\Phi\right) & \sigma_{\rho z} &= \frac{E}{1+\nu}\frac{\partial^2\Phi}{\partial\rho\partial z} \\
\sigma_{\rho\varphi} &= 0 & \sigma_{z\varphi} &= 0
\end{aligned} \tag{9}$$

The sum of the diagonal stress components become from Eqs. (9) and (7):

$$\sigma_{\rho\rho} + \sigma_{\varphi\varphi} + \sigma_{zz} = -\frac{2E}{1+\nu}\nabla^2\Phi \tag{10}$$

4 Temperature in the antisymmetric case

The temperature field due to the antisymmetric, infinite line heat source is obtained by integration of the well-known solution for an instantaneous point heat source along the z-axis. We have from Carslaw and Jaeger (1959):

$$T(x,y,z;t) = \int_{-\infty}^{\infty} \frac{q_0\ \mathrm{sign}(s)}{\rho_s c(4\pi a t)^{3/2}} \exp\left[-\frac{x^2+y^2+(z-s)^2}{4at}\right] ds \tag{11}$$

The volumetric heat capacity is $\rho_s c$ (J/m^{3}K), and a (m^2/s) denotes the thermal diffusivity of the solid.

With the substitution $u = \pm(s-z)/\sqrt{4at}$ for $s > 0$ and $s < 0$, respectively, we get:

$$T(\rho,z;t) = \frac{q_0}{\pi\rho_s c}\cdot\frac{1}{4at}\cdot e^{-\rho^2/(4at)}\,\mathrm{erf}\left(\frac{z}{\sqrt{4at}}\right) \tag{12}$$

The error function $\mathrm{erf}(z)$ and the complementary error function $\mathrm{erfc}(z)$ are given by, (Abramowitz and Stegun 1979):

$$\mathrm{erf}(z) = \frac{2}{\sqrt{\pi}}\int_0^z e^{-u^2}du = 1 - \mathrm{erfc}(z) \tag{13}$$

The error function increases from 0 for $z = 0$ to 1 for $z = \infty$.

The temperature field of the antisymmetric, infinite line heat source may be written in the following way:

$$T(\rho,z;t) = \frac{q_0}{\pi\rho_s c}\cdot\frac{1}{4at}\cdot T_a\left(\frac{\rho}{\sqrt{4at}}, \frac{z}{\sqrt{4at}}\right) \tag{14}$$

The field is, except for scale factors, given by the dimensionless temperature field $T_a(\rho', z')$ with the dimensionless coordinates of Eq. (19):

$$T_a(\rho', z') = e^{-(\rho')^2} \operatorname{erf}(z') \tag{15}$$

There is a single two-dimensional temperature field $T_a(\rho', z')$ for which the problem is to be solved. The dependence on time t involves scale factors only.

The dimensionless temperature field $T_a(\rho', z')$ is shown in Fig. 3. The temperature is an odd function of z', and it vanishes for $z' = 0$:

$$T_a(\rho', -z') = -T_a(\rho', z') \qquad T_a(\rho', 0) = 0 \tag{16}$$

For large z', T_a behaves as $e^{-(\rho')^2}$. We have the following asymptotic expressions:

$$T_a(\rho', z') \simeq e^{-(\rho')^2} \left(1 - \frac{1}{\sqrt{\pi} z'} e^{-(z')^2}\right) \qquad \text{for large } z' \tag{17}$$

$$T_a(\rho', z') \simeq \frac{2z'}{\sqrt{\pi}} \left(1 - (\rho')^2 - \frac{(z')^2}{3}\right) \qquad \text{for small } \rho',\ z' \tag{18}$$

5 Dimensionless formulation

The length $\sqrt{4at}$ is a measure of the thermal influence range from the line heat source at time t. This length, which is the only one occurring in the antisymmetric problem except the coordinates ρ and z, is used for the dimensionless coordinates:

$$\rho' = \frac{\rho}{\sqrt{4at}} \qquad z' = \frac{z}{\sqrt{4at}} \tag{19}$$

The dimensionless gradient and Laplace operators become:

$$\nabla = \frac{1}{\sqrt{4at}} \nabla' \qquad \nabla^2 = \frac{1}{4at} (\nabla')^2 \tag{20}$$

The displacement potential Φ satisfies Eq. (3) with T given by Eq. (14). Inserting the dimensionless Laplace operator, we get:

$$\frac{1}{4at} (\nabla')^2 \Phi = \frac{1+\nu}{1-\nu} \cdot \frac{\alpha q_0}{\pi \rho_s c} \cdot \frac{1}{4at} T_a(\rho', z') \tag{21}$$

The time factor $4at$ cancels. The displacement Φ becomes a function of ρ' and z' only:

$$\Phi(\rho, z, t) = \Phi_0 \cdot \Phi_a(\rho', z') \tag{22}$$

The scale factor Φ_0 (m^2) is given in Eq. (27).

The dimensionless displacement potential $\Phi_a(\rho', z')$ for the antisymmetric, infinite heat source is the solution of:

$$(\nabla')^2 \Phi_a = 2\, T_a(\rho', z') \tag{23}$$

The factor 2 on the right-hand side is introduced in order to avoid a numerical factor in Φ_a, Eq. (37).

The displacement $\mathbf{u}$ may now be written in the following form, Eq. (2):

$$\mathbf{u} = \frac{\Phi_0}{\sqrt{4at}} \cdot \mathbf{u}_a(\rho', z') \qquad \mathbf{u}_a = \nabla' \Phi_a \tag{24}$$

Here, $\mathbf{u}_a(\rho', z')$ is the dimensionless displacement. All functions with subscript $_a$ depend only on the dimensionless coordinates ρ' and z'.

The volume expansion e, Eq. (7), involves second derivatives (and $1/\rho$ times $\partial\Phi/\partial\rho$). This gives the scale factor $\Phi_0/(4at)$. From Eqs. (6) we get the same factor for the strain field. This factor is multiplied by $E/(1+\nu)$ for the stress field, Eq. (9):

$$e = \frac{\Phi_0}{4at} \cdot (\nabla')^2 \Phi_a \qquad \varepsilon = \frac{\Phi_0}{4at} \cdot \varepsilon_a(\rho', z') \qquad \sigma = \frac{F_0}{4at} \cdot \sigma_a(\rho', z') \tag{25}$$

Here, $\varepsilon_a(\rho', z')$ and $\sigma_a(\rho', z')$ denote the dimensionless strain and stress tensors. The stress scale factor F_0 (N) is given in Eq. (27). The components of the two tensors in the cylindrical coordinates are given by Eqs. (29) and (30).

The multiplicative scale factors, all with subscript $_0$, for displacement potential, displacement, strain, and stress, respectively, are:

$$\Phi_0 \quad (\mathrm{m}^2) \qquad \frac{\Phi_0}{\sqrt{4at}} \quad (\mathrm{m}) \qquad \frac{\Phi_0}{4at} \quad (\text{-}) \qquad \frac{F_0}{4at} \quad (\mathrm{N/m}^2) \tag{26}$$

The two scale constants Φ_0 and F_0 are defined by:

$$\Phi_0 = \frac{1+\nu}{1-\nu} \cdot \frac{\alpha q_0}{2\pi\rho_s c} \qquad F_0 = \frac{E\Phi_0}{1+\nu} = \frac{E\alpha q_0}{2\pi(1-\nu)\rho_s c} \tag{27}$$

The dimensionless displacements in the ρ'- and z'-directions are given by the partial derivatives of Φ_a, Eq. (24):

$$u_a(\rho', z') = \frac{\partial \Phi_a}{\partial \rho'} \qquad w_a(\rho', z') = \frac{\partial \Phi_a}{\partial z'} \tag{28}$$

The dimensionless strain components are now given by, Eqs. (6), (22), (19) and (25):

$$\varepsilon^a_{\rho\rho} = \frac{\partial^2 \Phi_a}{\partial(\rho')^2} \qquad \varepsilon^a_{\varphi\varphi} = \frac{1}{\rho'}\frac{\partial \Phi_a}{\partial \rho'} \qquad \varepsilon^a_{zz} = \frac{\partial^2 \Phi_a}{\partial(z')^2}$$

$$\varepsilon^a_{\rho z} = \frac{\partial^2 \Phi_a}{\partial \rho' \partial z'} \qquad \varepsilon^a_{\rho\varphi} = 0 \qquad \varepsilon^a_{z\varphi} = 0 \tag{29}$$

The dimensionless stress components are, Eqs. (9), (25) and(23):

$$\sigma^a_{\rho\rho} = \varepsilon^a_{\rho\rho} - 2\,T_a \qquad \sigma^a_{\varphi\varphi} = \varepsilon^a_{\varphi\varphi} - 2\,T_a \qquad \sigma^a_{zz} = \varepsilon^a_{zz} - 2\,T_a$$

$$\sigma^a_{\rho z} = \varepsilon^a_{\rho z} \qquad \sigma^a_{\rho\varphi} = 0 \qquad \sigma^a_{z\varphi} = 0 \tag{30}$$

The sum of the diagonal components becomes from Eqs. (29), (23) and (30):

$$\varepsilon^a_{\rho\rho} + \varepsilon^a_{\varphi\varphi} + \varepsilon^a_{zz} = 2\,T_a \qquad \sigma^a_{\rho\rho} + \sigma^a_{\varphi\varphi} + \sigma^a_{zz} = -4\,T_a \tag{31}$$

These dimensionless equations correspond to the original equations (7) and (10), respectively.

6 Displacement potential Φ_a

The displacement potential $\Phi_a(\rho', z')$ satisfies Eq. (23), which together with Eq. (15) gives:

$$(\nabla')^2 \Phi_a = 2\, T_a(\rho', z') = 2e^{-(\rho')^2} \operatorname{erf}(z') \tag{32}$$

The solution $\Phi_a(\rho', z')$ is according to Eqs. (4) and (16) an odd function of z', so that it vanishes for $z' = 0$:

$$\Phi_a(\rho', 0) = 0 \tag{33}$$

A solution is readily obtained by taking the derivative of Eq. (32) with respect to z' for constant ρ':

$$(\nabla')^2 \left[\left(\frac{\partial \Phi_a}{\partial z'} \right)_{\rho'} \right] = 2e^{-(\rho')^2} \cdot \frac{2}{\sqrt{\pi}} e^{-(z')^2} = \frac{4}{\sqrt{\pi}} e^{-(r')^2} \tag{34}$$

Here, r' is the dimensionless radial distance in spherical coordinates. The right-hand side, and hence $\partial \Phi_a / \partial z'$, is a function of r' only. The Laplace operator, with radial variation only, gives:

$$\frac{1}{r'} \frac{d^2}{d(r')^2} \left[r' \left(\frac{\partial \Phi_a}{\partial z'} \right)_{\rho'} \right] = \frac{4}{\sqrt{\pi}} e^{-(r')^2} \tag{35}$$

Integration gives:

$$\left(\frac{\partial \Phi_a}{\partial z'} \right)_{\rho'} = -\frac{\operatorname{erf}(r')}{r'} + A + \frac{B}{r'} = -\frac{\operatorname{erf}\left(\sqrt{(\rho')^2 + (z')^2} \right)}{\sqrt{(\rho')^2 + (z')^2}} \tag{36}$$

Here, A and B are integration constants. The solution is regular at $r' = 0$, which means that B is zero, since $\operatorname{erf}(r')/r'$ is regular for $r' = 0$. The constant A corresponds to a constant displacement in the z-direction. This part will vanish for the finite line heat source, which involves a difference of two antisymmetric cases. It is therefore of no importance, and we put A to zero. Equation (36) gives a particular solution to Eq. (32). To this any solution to the homogeneous equation $\nabla^2 \Phi = 0$ may be added. Separation of variables gives solutions such as $e^{\beta z'} \mathrm{J}_0(\beta \rho')$, but these solutions are discarded, since the gradient is infinite for infinite exponents.

The dimensionless displacement potential for the infinite, antisymmetric line heat source is now by integration from $s = 0$ to $s = z'$, with $\Phi_a(\rho', 0)$ equal to zero according to Eq. (33):

$$\Phi_a(\rho', z') = -\int_0^{z'} \frac{\operatorname{erf}\left(\sqrt{(\rho')^2 + s^2} \right)}{\sqrt{(\rho')^2 + s^2}}\, ds \tag{37}$$

The expression is valid for all ρ' and z'.

The displacement potential $\Phi_a(\rho', z')$ is without difficulty calculated numerically from Eq. (37). The result is shown in Fig. 4. The potential is an odd function of z'. The values on the axes are, Eqs. (33) and (37):

$$\Phi_a(\rho', 0) = 0 \qquad \Phi_a(0, z') = -\int_0^{z'} \frac{\operatorname{erf}(s)}{s}\, ds \tag{38}$$

The behavior along the z'-axis is shown in Fig. 5. The potential $-\Phi_a(0,z')$ increases towards infinity as $\ln(z')$ for large positive z'. Asymptotic expressions for small, Eq. (117), and for large z', Eq. (115), are also shown.

7 Displacement field

A simple way to obtain the radial displacement u_a is to use Eq. (37) after the substitution $s = \rho' v$. We have:

$$u_a = -\frac{\partial}{\partial \rho'} \left[\int_0^{z'/\rho'} \frac{\operatorname{erf}\left(\rho' \sqrt{1+v^2}\right)}{\sqrt{1+v^2}} dv \right] \tag{39}$$

The factor $\sqrt{1+v^2}$ cancels after derivation in the integral, and we get after straightforward calculations:

$$u_a = \frac{1}{\rho'} \left[\frac{z'}{r'} \operatorname{erf}(r') - e^{-(\rho')^2} \operatorname{erf}(z') \right] \tag{40}$$

Derivation of Eq. (37) with respect to z' gives directly:

$$w_a = -\frac{\operatorname{erf}(r')}{r'} \qquad r' = \sqrt{(\rho')^2 + (z')^2} \tag{41}$$

The displacement $u_a(\rho', z')$, Eq. (40), is an odd function of z'. In order to determine the behavior for $\rho' = 0$, we consider the function within the brackets in Eq. (40). The series expansion in ρ' for fixed z' becomes:

$$\frac{z'}{r'} \operatorname{erf}(r') - e^{-(\rho')^2} \operatorname{erf}(z') = 0 + \rho' \cdot 0 + (\rho')^2 \cdot \left[\operatorname{erf}(z') \left(1 - \frac{1}{2(z')^2} \right) + \frac{1}{\sqrt{\pi} z'} e^{-(z')^2} \right] + \ldots \tag{42}$$

The function on the left-hand side and its first derivative with respect to ρ' vanish for $\rho' = 0$. The radial displacement near $\rho' = 0$ becomes from Eqs. (42) and (40):

$$u_a(\rho', z') = \rho' \cdot e_2(z') + (\rho')^2 \cdot [\ldots] \tag{43}$$

Here, $e_2(z')$ denotes the function within the brackets in Eq. (42). It is given below by Eq. (53).

From Eqs. (40) and (43) we get that u_a is zero on both axis:

$$u_a(\rho', 0) = 0 \qquad u_a(0, z') = 0 \tag{44}$$

In the limit $z' = \infty$, we get from Eq. (40):

$$u_a(\rho', \infty) = \frac{1 - e^{-(\rho')^2}}{\rho'} \tag{45}$$

This function together with asymptotic expressions is shown in Fig. 6. The function assumes the maximum 0.6382 for $\rho' = 1.1209$. The radial displacement field $u_a(\rho', z')$ is shown in Fig. 7.

The displacement $w_a(\rho', z')$, Eq. (41), in the z-direction depends of the radius r' only. The function $\operatorname{erf}(r')/r'$ together with asymptotic behavior is shown in Fig. 8. The

curves of constant w_a are circles in the (ρ', z')-plane. The largest vertical (downward) displacement $2/\sqrt{\pi} = 1.128$ occurs at $r' = 0$.

The displacement vector field $\mathbf{u}_a$ may from Eqs. (5), (40) and (41) be written in the following way:

$$\mathbf{u}_a = \frac{1}{\rho'}\left(\mathrm{erf}(r')\,\mathbf{e}_\theta - e^{-(\rho')^2}\mathrm{erf}(z')\,\mathbf{e}_\rho\right) \tag{46}$$

Here, $\mathbf{e}_\theta$ is the unit vector in the θ-direction, Fig. 2:

$$\mathbf{e}_\theta = \cos(\theta)\,\mathbf{e}_\rho - \sin(\theta)\,\mathbf{e}_z \tag{47}$$

The displacement vector field is shown in Fig. 9.

8 Strain field

The components of the strain tensor ε_a are given by second-order derivatives of Φ_a, Eqs. (29), or first order derivatives of the displacement components u_a and w_a, Eqs. (28). We get with straightforward derivations from Eqs. (40) and (41):

$$\varepsilon^a_{\rho\rho} = -\frac{z'}{r'}\cdot\frac{1}{(r')^2}\left[\mathrm{erf}(r') - \frac{2r'}{\sqrt{\pi}}e^{-(r')^2}\right] - \frac{1}{(\rho')^2}\left[\frac{z'}{r'}\mathrm{erf}(r') - e^{-(\rho')^2}\mathrm{erf}(z')\right] + 2e^{-(\rho')^2}\,\mathrm{erf}(z')$$

$$\varepsilon^a_{\varphi\varphi} = \frac{1}{(\rho')^2}\left[\frac{z'}{r'}\mathrm{erf}(r') - e^{-(\rho')^2}\mathrm{erf}(z')\right]$$

$$\varepsilon^a_{zz} = \frac{z'}{r'}\cdot\frac{1}{(r')^2}\left[\mathrm{erf}(r') - \frac{2r'}{\sqrt{\pi}}e^{-(r')^2}\right]$$

$$\varepsilon^a_{\rho z} = \frac{\rho'}{r'}\cdot\frac{1}{(r')^2}\left[\mathrm{erf}(r') - \frac{2r'}{\sqrt{\pi}}e^{-(r')^2}\right] \tag{49}$$

These four strain components are shown in Fig. 10.

The last two strain components differ only by the factors z' and ρ'. They may be written, Fig. 2:

$$\varepsilon^a_{zz} = \cos(\theta)\; e_1(r') \qquad \varepsilon^a_{\rho z} = \sin(\theta)\; e_1(r') \tag{50}$$

Here, the function $e_1(r')$ is given by:

$$e_1(r') = \frac{1}{(r')^2}\left[\mathrm{erf}(r') - \frac{2r'}{\sqrt{\pi}}e^{-(r')^2}\right] \tag{51}$$

This function is shown in Fig. 11. It attains the maximum 0.428 at r'=0.97. Asymptotes for large and small r' are shown.

The strain $\varepsilon^a_{\varphi\varphi}$ in the rotational direction φ is zero on the ρ'-axis. It is directly related to u_a, Eqs. (28-29):

$$\varepsilon^a_{\varphi\varphi} = \frac{1}{\rho'}\frac{\partial\Phi_a}{\partial\rho'} = \frac{u_a}{\rho'} \tag{52}$$

The expressions for $\varepsilon^a_{\varphi\varphi}$ have ρ' in the denominator, so values for $\rho' = 0$ are not directly obtainable. But from Eq. (43) we have after division by ρ' for $\rho' = 0$:

$$\varepsilon^a_{\varphi\varphi}(0, z') = e_2(z')$$

$$e_2(z') = \mathrm{erf}(z') \left(1 - \frac{1}{2(z')^2}\right) + \frac{1}{\sqrt{\pi} z'} e^{-(z')^2} \tag{53}$$

The function $e_2(z')$ is shown in Fig. 12. The limit of infinite z' is of interest. We have in accordance with (83):

$$\varepsilon^a_{\varphi\varphi}(\rho', \infty) = \frac{1 - e^{-(\rho')^2}}{(\rho')^2} \tag{54}$$

This function is shown by curve II in Fig. 14.

The expression for $\varepsilon^a_{\rho\rho}$ in Eqs. (49) is somewhat more complicated than the other three expressions. But we have from Eq. (31):

$$\varepsilon^a_{\rho\rho} = -\varepsilon^a_{zz} - \varepsilon^a_{\varphi\varphi} + 2\, T_a \tag{55}$$

The values on the axes become:

$$\varepsilon^a_{\rho\rho}(\rho', 0) = 0 \qquad \varepsilon^a_{\rho\rho}(0, z') = e_2(z') \tag{56}$$

For the second equation, we have used Eq. (55) (or the fact that $\varepsilon^a_{\rho\rho}$ and $\varepsilon^a_{\varphi\varphi}$ must be equal on the z'-axis).

The strain component $\varepsilon^a_{\rho\rho}$ is the derivative of $u_a(\rho', z')$ with respect to ρ', Eqs. (28-29). The vertical curve $\varepsilon^a_{\rho\rho} = 0$ in Fig. 10, top left, corresponds to the maximum $(\partial u_a / \partial \rho')_{z'} = 0$ in Fig. 7.

9 Stress field

The components of stress field are directly obtained from the strain components and T_a, Eqs. (30). Using Eqs. (49) and (15), we get:

$$\begin{aligned}
\sigma^a_{\rho\rho} &= -\frac{z'}{r'} \cdot \frac{1}{(r')^2} \left[\mathrm{erf}(r') - \frac{2r'}{\sqrt{\pi}} e^{-(r')^2}\right] - \frac{1}{(\rho')^2} \left[\frac{z'}{r'} \mathrm{erf}(r') - e^{-(\rho')^2} \mathrm{erf}(z')\right] \\
\sigma^a_{\varphi\varphi} &= \frac{1}{(\rho')^2} \left[\frac{z'}{r'} \mathrm{erf}(r') - e^{-(\rho')^2} \mathrm{erf}(z')\right] - 2e^{-(\rho')^2} \mathrm{erf}(z') \\
\sigma^a_{zz} &= \frac{z'}{r'} \cdot \frac{1}{(r')^2} \left[\mathrm{erf}(r') - \frac{2r'}{\sqrt{\pi}} e^{-(r')^2}\right] - 2e^{-(\rho')^2} \mathrm{erf}(z') \\
\sigma^a_{\rho z} &= \frac{\rho'}{r'} \cdot \frac{1}{(r')^2} \left[\mathrm{erf}(r') - \frac{2r'}{\sqrt{\pi}} e^{-(r')^2}\right]
\end{aligned} \tag{57}$$

These four non-vanishing components of the stress tensor are shown in Fig. 13.

The first three components $\sigma^a_{\rho\rho}$, $\sigma^a_{\varphi\varphi}$ and σ^a_{zz} are odd functions of z', while $\sigma^a_{\rho z}$ is even in z'. The component $\sigma^a_{\rho\rho}$ assumes negative values and $\sigma^a_{\rho z}$ positive values for $z' > 0$. The second and third components $\sigma^a_{\varphi\varphi}$ and σ^a_{zz} are negative near the positive z'-axis (compression) and positive (tension) in a region outside $\rho' = 1$.

Let us further consider the first three components $\sigma^a_{\rho\rho}$, $\sigma^a_{\varphi\varphi}$ and σ^a_{zz}. They are all zero on the ρ'-axis. On the z'-axis, we have from Eqs. (30), (56) and (15):

$$\sigma^a_{\rho\rho}(0, z') = e_2(z') - 2\,\mathrm{erf}(z') = -e_3(z') \tag{58}$$

From Eqs. (30), (53), and (15) we have in the same way:

$$\sigma^a_{\varphi\varphi}(0,z') = -e_3(z') \tag{59}$$

It should be noted that $\sigma^a_{\rho\rho}$ and $\sigma^a_{\varphi\varphi}$ must be equal for $\rho' = 0$. The function $e_3(z')$ is given by, Eqs. (53) and (58):

$$e_3(z') = \operatorname{erf}(z')\left(1 + \frac{1}{2(z')^2}\right) - \frac{1}{\sqrt{\pi}z'}e^{-(z')^2} \tag{60}$$

This function is shown in Fig. 12. It is an odd function of z'. The maximum is of interest since it gives the largest compression for $\sigma^a_{\rho\rho}$ and $\sigma^a_{\varphi\varphi}$:

$$e_{3,\max} = 1.141 \quad \text{for} \quad z' = 1.51 \tag{61}$$

From Eqs. (57), (51) and (53) we get:

$$\sigma^a_{zz}(0,z') = e_1(z') - 2\operatorname{erf}(z') = -2e_2(z') \tag{62}$$

The compression increases along the positive z'-axis from zero to $+2$ for $z' = \infty$. There is a local maximum $\sigma^a_{zz} = 0.064$ at the point $\rho' = 2.2$, $z' = 1.5$. See Fig. 13 bottom, left.

The behavior on the z'-axis is summarized in Fig. 12. We have from the above equations:

$$\sigma^a_{\rho\rho}(0,z') = \sigma^a_{\varphi\varphi}(0,z') = -e_3(z') \qquad \sigma^a_{zz}(0,z') = -2e_2(z') \qquad \sigma^a_{\rho z}(0,z') = 0 \tag{63}$$

The behavior for large z' is of interest. For $z' = \infty$, we have from Eqs. (57):

$$\sigma^a_{\rho\rho}(\rho',\infty) = -\frac{1}{(\rho')^2}\left[1 - e^{-(\rho')^2}\right] \qquad \sigma^a_{zz}(\rho',\infty) = -2e^{-(\rho')^2}$$

$$\sigma^a_{\varphi\varphi}(\rho',\infty) = \frac{1}{(\rho')^2}\left[1 - e^{-(\rho')^2}\right] - 2e^{-(\rho')^2} \qquad \sigma^a_{\rho z}(\rho',\infty) = 0 \tag{64}$$

These three functions of ρ' are shown in Fig. 14. The component $\sigma^a_{\varphi\varphi}(\rho',\infty)$ (curve III) is zero for $\rho' = 1.121$. The stress is negative for $0 < \rho' < 1.121$ and positive for $\rho' > 1.121$ in accordance with Fig. 13, top left. There is a stress maximum $\sigma^a_{\varphi\varphi} = 0.218$ for $\rho' = 1.793$, $z' = \infty$.

We have obtained the following maxima and minima in $z' > 0$ for the first three components:

$$\begin{aligned}
\sigma^a_{\rho\rho,\min} &= -1.14 \quad \text{for} \quad \rho' = 0,\ z' = 1.51 \\
\sigma^a_{\varphi\varphi,\min} &= -1.14 \quad \text{for} \quad \rho' = 0,\ z' = 1.51 \\
\sigma^a_{\varphi\varphi,\max} &= 0.218 \quad \text{for} \quad \rho' = 1.79,\ z' = \infty \\
\sigma^a_{zz,\min} &= -2 \quad \text{for} \quad \rho' = 0,\ z' = \infty \\
\sigma^a_{zz,\max} &= 0.064 \quad \text{for} \quad \rho' = 2.2,\ z' = 1.5
\end{aligned} \tag{65}$$

The shear stress $\sigma^a_{\rho z} = \varepsilon^a_{\rho z}$, Fig. 13 (bottom right), has a different character. It is an even function of z' and zero on the z'-axis. We have from Eq. (50):

$$\sigma^a_{\rho z}(\rho',z') = \sin(\theta)e_1(r') \tag{66}$$

The function $e_1(r')$, Eq. (51), is shown in Fig. 11. On the ρ'-axis, $\sigma^a_{\rho z}$ is equal to $e_1(\rho')$. The maximum of e_1 gives the maximum shear stress:

$$\sigma^a_{\rho z,max} = 0.428 \quad \text{for} \quad \rho' = 0.97,\ z' = 0 \tag{67}$$

With the use of $e_1(r')$, $\varepsilon^a_{\varphi\varphi}(\rho', z')$ and $T_a(\rho', z')$, the stress components, Eqs. (57), may be written in the following more compact form:

$$\begin{aligned} \sigma^a_{\rho\rho} &= -\cos(\theta) \cdot e_1(r') - \varepsilon^a_{\varphi\varphi}(\rho', z') \\ \sigma^a_{\varphi\varphi} &= \varepsilon^a_{\varphi\varphi}(\rho', z') - 2T_a(\rho', z') \\ \sigma^a_{zz} &= \cos(\theta) \cdot e_1(r') - 2T_a(\rho', z') \\ \sigma^a_{\rho z} &= \sin(\theta) \cdot e_1(r') \end{aligned} \tag{68}$$

The function $e_1(r')$, Eq. (51), is shown in Fig. 11, the dimensionless temperature $T_a(\rho', z')$, Eq. (15), in Fig. 3, and $\varepsilon^a_{\varphi\varphi}(\rho', z')$, Eq. (49) in Fig. 10 (top right).

10 Principal stresses

The dimensionless principal stresses, denoted σ^a_1, σ^a_2 and σ^a_3, are readily computed from the expressions (57). The shear stresses for φ-surfaces, $\sigma_{\rho\varphi}$ and $\sigma_{z\varphi}$, are zero, Eq. (9). Thus, $\sigma^a_{\varphi\varphi}$ is a principal stress:

$$\sigma^a_3 = \sigma^a_{\varphi\varphi} \tag{69}$$

Figure 13, top right, shows this stress field. The three stress components in the (ρ', z')-plane determine the other two principal stresses. The well known formula for the normal stresses is:

$$\sigma^a_{1,2} = \frac{\sigma^a_{\rho\rho} + \sigma^a_{zz}}{2} \mp \sqrt{\left(\frac{\sigma^a_{zz} - \sigma^a_{\rho\rho}}{2}\right)^2 + \left(\sigma^a_{\rho z}\right)^2} \tag{70}$$

Here, σ^a_2 has the plus sign before the square root. The stress components $\sigma^a_{\rho\rho}$ and σ^a_{zz} are odd functions of z', while $\sigma^a_{\rho z}$ is even in z'. Then we have from Eq. (70):

$$\sigma^a_2(\rho', z') = -\sigma^a_1(\rho', -z') \tag{71}$$

Let θ_1 denote the angle between the first principal stress direction and the z'-axis. We have:

$$\tan(2\theta_1) = \frac{2\sigma^a_{\rho z}}{\sigma^a_{\rho\rho} - \sigma^a_{zz}} \tag{72}$$

Figure 15 shows the principal stresses in the (ρ', z')-plane. The plane is divided into three areas by the dashed lines. There is compression in both principal directions in the upper area, and tension in both directions in the lower area. In the intermediate area in a sector around the ρ'-axis, there is compression in the direction top-left to bottom-right. This principal compression decreases from the upper dashed line down to the lower one, where the compression becomes zero. In the other principal direction from bottom-right to top-left there is tension in the intermediate area. This tension decreases from the lower dashed line to zero on the upper line.

The shear stress $\sigma^a_{\rho z}$ is zero on the z'-axis. The two principal stresses and the angle to the z'-axis become from Eqs. (63) and (71) for $z > 0$:

$$\sigma^a_1(0, z') = \sigma^a_{zz}(0, z') = -2e_2(z') \qquad z' > 0$$

$$\sigma_2^a(0,z') = \sigma_{\rho\rho}^a(0,z') = -e_3(z') \qquad z' > 0$$
$$\theta_1(0,z') = 0 \tag{73}$$

On the ρ'-axis we have, Eq. (66) with $\theta = \pi/2$:

$$\sigma_{\rho\rho}^a(\rho',0) = 0 \qquad \sigma_{zz}^a(\rho',0) = 0 \qquad \sigma_{\rho z}^a(\rho',0) = e_1(\rho') \tag{74}$$

This gives

$$\sigma_1^a(\rho',0) = -\sigma_2^a(\rho',0) = -e_1(\rho') \qquad \theta_1(\rho',0) = \pi/4 \tag{75}$$

The dashed curves in Fig. 15, where one of the principal stresses are zero, are determined by the condition:

$$\sigma_{\rho\rho}^a \cdot \sigma_{zz}^a = \left(\sigma_{\rho z}^a\right)^2 \tag{76}$$

The behavior for small r' is discussed in Appendix 2. The dashed curves follow the lines $z' = \pm\rho'/2$ for small r', Eq. (122).

11 Asymptotic behavior

We are interested in the behavior of the solution for large r', and in particular for large z' and moderate ρ' near the z'-axis where the line heat source lies. The asymptotic behavior of the displacement potential Φ_a for large radius r' is dealt with in more detail in Appendix 1.

Eqs. (40-41) for the displacements can be simplified for large r'. The error function $\mathrm{erf}(r')$ is close to unity (erf(2)=0.995, erf(1.4)=0.95). For $r' > 2$, we have with good accuracy:

$$\mathrm{erf}(r') \simeq 1 \qquad r'e^{-(r')^2} \simeq 0$$
$$e^{-(\rho')^2}[1 - \mathrm{erf}(z')] \simeq 0 \quad \text{or} \quad e^{-(\rho')^2}\mathrm{erf}(z') \simeq e^{-(\rho')^2} \qquad (r' > 2,\ z' > 0) \tag{77}$$

The equation in the second line is directly valid for $z' > 2$. But ρ' becomes large for small z' (and $r' > 2$). Then the exponential is small.

With these approximations, the displacement becomes:

$$u_a \simeq \frac{1}{\rho'}\left[\frac{z'}{r'} - e^{-(\rho')^2}\right] \qquad w_a \simeq -\frac{1}{r'} \qquad (r' > 2) \tag{78}$$

The strain components, Eqs. (49), become:

$$\varepsilon_{\rho\rho}^a \simeq -\frac{z'}{(r')^3} - \frac{1}{(\rho')^2}\left[\frac{z'}{r'} - e^{-(\rho')^2}\right] + 2e^{-(\rho')^2} \qquad \varepsilon_{zz}^a \simeq \frac{z'}{(r')^3}$$
$$\varepsilon_{\varphi\varphi}^a \simeq \frac{1}{(\rho')^2}\left[\frac{z'}{r'} - e^{-(\rho')^2}\right] \qquad \varepsilon_{\rho z}^a \simeq \frac{\rho'}{(r')^3} \qquad (r' > 2,\ z' > 0) \tag{79}$$

The stress components, Eqs. (57), become in the same approximation:

$$\sigma_{\rho\rho}^a \simeq -\frac{z'}{(r')^3} - \frac{1}{(\rho')^2}\left[\frac{z'}{r'} - e^{-(\rho')^2}\right] \qquad \sigma_{zz}^a \simeq \frac{z'}{(r')^3} - 2e^{-(\rho')^2}$$

$$\sigma^a_{\varphi\varphi} \simeq \frac{1}{(\rho')^2}\left[\frac{z'}{r'} - e^{-(\rho')^2}\right] - 2e^{-(\rho')^2} \qquad \sigma^a_{\rho z} \simeq \frac{\rho'}{(r')^3} \qquad (r' > 2,\ z' > 0) \tag{80}$$

The limit $z' = \infty$ is also of interest. It gives the two-dimensional behavior around an infinite line heat source. In this limit we have:

$$\frac{z'}{r'} = 1 \qquad r' = \infty \qquad \mathrm{erf}(z') = 1 \qquad (z' = \infty) \tag{81}$$

With these approximations, the displacement becomes, in accordance with Eq. (45):

$$u_a = \frac{1}{\rho'}\left[1 - e^{-(\rho')^2}\right] \qquad w_a = 0 \qquad (z' = \infty) \tag{82}$$

The strain components, Eqs. (49), become:

$$\varepsilon^a_{\rho\rho} = -\frac{1}{(\rho')^2}\left[1 - e^{-(\rho')^2}\right] + 2e^{-(\rho')^2} \qquad \varepsilon^a_{zz} = 0$$

$$\varepsilon^a_{\varphi\varphi} = \frac{1}{(\rho')^2}\left[1 - e^{-(\rho')^2}\right] \qquad \varepsilon^a_{\rho z} = 0 \qquad (z' = \infty) \tag{83}$$

The stress components, Eqs. (57), for the limit $z' = \infty$ are given previously in Eqs. (64). The three nonzero stress components are shown in Fig. 14. It may be noted that the same functions occur in Eqs. (64) for stresses and Eqs. (83) for strains. The three curves in Fig. 14 show:

$$\begin{aligned} &\text{curve I:} && -\sigma^a_{zz}(\rho', \infty) \\ &\text{curve II:} && -\sigma^a_{\rho\rho}(\rho', \infty) = \varepsilon^a_{\varphi\varphi}(\rho', \infty) \\ &\text{curve III:} && -\sigma^a_{\varphi\varphi}(\rho', \infty) = \varepsilon^a_{\rho\rho}(\rho', \infty) \end{aligned} \tag{84}$$

The limit $z' = \infty$ gives the two-dimensional radial solution from an infinite line source with the (dimensionless) temperature, Eq. (15):

$$T = e^{-(\rho')^2} \cdot 1 \tag{85}$$

Let us verify this. The (plane) radial displacement potential $\Phi'(\rho')$ is the solution of Eq. (23):

$$(\nabla')^2\Phi' = \frac{1}{\rho'}\frac{d}{d\rho'}\left(\rho'\frac{d\Phi'}{d\rho'}\right) = 2e^{-(\rho')^2} \tag{86}$$

The solution is regular at $\rho' = 0$, and we get after two integrations:

$$\Phi' = \ln(\rho') + 0.5\,\mathrm{E}_1\left((\rho')^2\right) \tag{87}$$

Here, E_1 denotes the exponential integral, Eq. (110). The derivative $d\Phi'/d\rho'$ gives the displacement u_a in accordance with Eq. (82). Second derivatives, Eqs. (29-30), give the strain and stress in accordance with Eqs. (83) and (64).

Far away from the line source, $\rho' > 2$ and $r' > 2$, we can neglect the exponential in $(\rho')^2$. The displacement (78) is simplified to:

$$u_a \simeq \frac{z'}{\rho' r'} \qquad w_a \simeq -\frac{1}{r'} \qquad (\rho', z' > 2) \tag{88}$$

The strain and stress become equal, since T_a and $(\nabla')^2\Phi_a$ are zero in this approximation, and we have from Eqs. (79-80):

$$\sigma^a_{\rho\rho} \simeq \varepsilon^a_{\rho\rho} \simeq -\frac{z'}{r'}\left[\frac{1}{(\rho')^2}+\frac{1}{r'^2}\right] \qquad \sigma^a_{\varphi\varphi} \simeq \varepsilon^a_{\varphi\varphi} \simeq \frac{z'}{r'(\rho')^2}$$

$$\sigma^a_{zz} \simeq \varepsilon^a_{zz} \simeq \frac{z'}{(r')^3} \qquad \sigma^a_{\rho z} = \varepsilon^a_{\rho z} \simeq \frac{\rho'}{(r')^3} \qquad (\rho', r' > 2) \tag{89}$$

12 Development with time

The original displacement field $\mathbf{u}(\rho, z, t)$ (m) becomes from Eqs. (24), (19), (40) and (41):

$$u(\rho,z,t) = \frac{\Phi_0}{\rho}\left[\frac{z}{r}\,\mathrm{erf}\left(\frac{r}{\sqrt{4at}}\right) - e^{-\rho^2/(4at)}\,\mathrm{erf}\left(\frac{z}{\sqrt{4at}}\right)\right]$$

$$w(\rho,z,t) = -\frac{\Phi_0}{r}\mathrm{erf}\left(\frac{r}{\sqrt{4at}}\right) \tag{90}$$

The original stress components (Pa) become from Eqs. (57), (25) and (19):

$$\begin{aligned}
\sigma_{\rho\rho}(\rho,z,t) &= -F_0\left\{\frac{z}{r^3}\left[\mathrm{erf}\left(\frac{r}{\sqrt{4at}}\right) - \frac{2}{\sqrt{\pi}}\frac{r}{\sqrt{4at}}e^{-r^2/(4at)}\right] + \right. \\
&\qquad \left. + \frac{1}{\rho^2}\left[\frac{z}{r}\,\mathrm{erf}\left(\frac{r}{\sqrt{4at}}\right) - e^{-\rho^2/(4at)}\mathrm{erf}\left(\frac{z}{\sqrt{4at}}\right)\right]\right\} \\
\sigma_{\varphi\varphi}(\rho,z,t) &= F_0\left\{\frac{1}{\rho^2}\left[\frac{z}{r}\,\mathrm{erf}\left(\frac{r}{\sqrt{4at}}\right) - e^{-\rho^2/(4at)}\mathrm{erf}\left(\frac{z}{\sqrt{(4at)}}\right)\right] - \frac{2}{4at}e^{-\rho^2/(4at)}\mathrm{erf}\left(\frac{z}{\sqrt{4at}}\right)\right\} \\
\sigma_{zz}(\rho,z,t) &= F_0\left\{\frac{z}{r^3}\left[\mathrm{erf}\left(\frac{r}{\sqrt{4at}}\right) - \frac{2}{\sqrt{\pi}}\frac{r}{\sqrt{4at}}e^{-r^2/(4at)}\right] - \frac{2}{4at}e^{-\rho^2/(4at)}\mathrm{erf}\left(\frac{z}{\sqrt{4at}}\right)\right\} \\
\sigma_{\rho z}(\rho,z,t) &= F_0\frac{\rho}{r^3}\left[\mathrm{erf}\left(\frac{r}{\sqrt{4at}}\right) - \frac{2}{\sqrt{\pi}}\frac{r}{\sqrt{4at}}e^{-r^2/(4at)}\right]
\end{aligned} \tag{91}$$

13 Finite line source

We will in this section briefly consider the finite line heat source. The heat source lies along the z-axis in the finite interval $z_- < z < z_+$. The heat q_0 (J/m) is released at $t = 0$. See Fig. 1B. The total amount of released heat is $(z_+ - z_-)\,q_0$ (J). This heat source may be obtained from two superimposed infinite antisymmetric cases. The first one has the strength $q_0/2$ (J/m) and its center at $z = z_-$. The other one has the strength $-q_0/2$ (J/m) and the center at $z = z_+$. The heat release along the z-axis at $t = 0$ becomes:

$$\frac{q_0}{2}\cdot\mathrm{sign}(z-z_-) - \frac{q_0}{2}\cdot\mathrm{sign}(z-z_+) = \begin{cases} 0 & z > z_+ \\ q_0 & z_- < z < z_+ \\ 0 & z < z_- \end{cases} \tag{92}$$

The temperature for an infinite antisymmetric line source is given by Eq. (14). By superposition we have for the finite line source:

$$T(\rho,z,t)=\frac{1}{2}\cdot\frac{q_0}{\pi\rho_s c}\cdot\frac{1}{4at}\cdot\left[T_a\left(\frac{\rho}{\sqrt{4at}},\frac{z-z_-}{\sqrt{4at}}\right)-T_a\left(\frac{\rho}{\sqrt{4at}},\frac{z-z_+}{\sqrt{4at}}\right)\right] \tag{93}$$

The displacement potential is the solution of Eq. (3) with T given by the above expression with its two parts. We get by superposition:

$$\Phi(\rho,z,t)=\Phi_0\cdot\tfrac{1}{2}\left[\Phi_a(\rho',z'-z'_-)-\Phi_a(\rho',z'-z'_+)\right]\qquad z'_\pm=z_\pm/\sqrt{(4at)} \tag{94}$$

Here, z'_+ and z'_- are the dimensionless top and bottom positions of the line source.

The displacement vector, and the strain and stress tensors, are readily obtained by the above type of superposition. For example, we have for the dimensionless stress tensor:

$$\sigma'(\rho',z';z'_+,z'_-)=\tfrac{1}{2}\left[\sigma^a(\rho',z'-z'_-)-\ \sigma^a(\rho',z'-z'_+)\right] \tag{95}$$

The four nonzero components of the dimensionless stress tensor $\sigma^a(\rho',z')$ are given by Eqs. (57). For example, we have for the σ'_{zz}-component:

$$\sigma'_{zz}(\rho',z';z'_+,z'_-)=\frac{1}{2}\left\{\frac{z'-z'_-}{(r'_-)^3}\left[\mathrm{erf}(r'_-)-\frac{2r'_-}{\sqrt{\pi}}e^{-(r'_-)^2}\right]\right.$$

$$\left.-\frac{z'-z'_+}{(r'_+)^3}\left[\mathrm{erf}(r'_+)-\frac{2r'_+}{\sqrt{\pi}}e^{-(r'_+)^2}\right]-2e^{-(\rho')^2}\left[\mathrm{erf}(z'-z'_-)-\mathrm{erf}(z'-z'_+)\right]\right\} \tag{96}$$

Here, the dimensionless distances to top and bottom of the line source are:

$$r'_+=\sqrt{(\rho')^2+(z'-z'_+)^2}\qquad r'_-=\sqrt{(\rho')^2+(z'-z'_-)^2} \tag{97}$$

We now choose $z=0$ as the midpoint of the line source with the length H:

$$z_+=H/2\qquad z_-=-H/2\qquad z'_\pm=\pm H'(t)\qquad H'(t)=\frac{H}{2\sqrt{4at}} \tag{98}$$

Then the dimensionless stress field σ' depends on the dimensionless coordinates ρ' and z' and on the dimensionless *half*-length H' of the line source:

$$\sigma'(\rho',z';H')=\tfrac{1}{2}\left[\sigma^a(\rho',z'+H')-\ \sigma^a(\rho',z'-H')\right] \tag{99}$$

Figure 16 shows the four nonzero components for the particular case $H'=10$. This means that H is twenty times larger than the thermal range $\sqrt{4at}$, Eq. (98).

14 Time-dependent heat source

Let $\mathrm{sign}(z)q_0\,q'(t)$ (W/m) be a *time-dependent* antisymmetric heat source along the z-axis. The variation in time is given by the dimensionless function $q'(t)$. The temperature is obtained from Duhamel's superposition theorem (Carslaw and Jaeger 1959) as an integral of the instantaneous heat source solution, Eq. (14):

$$T(\rho,z,t)=\int_0^t q'(t')\cdot\frac{q_0}{\pi\rho_s c}\cdot\frac{1}{4a(t-t')}\cdot T_a\left(\frac{\rho}{\sqrt{4a(t-t')}},\frac{z}{\sqrt{4a(t-t')}}\right)dt' \tag{100}$$

Here, $T_a(\rho', z')$ is given by Eq. (15). The displacement potential is in the same way given by:

$$\Phi(\rho, z, t) = \Phi_0 \int_0^t q'(t')\, \Phi_a \left(\frac{\rho}{\sqrt{4a(t-t')}}, \frac{z}{\sqrt{4a(t-t')}} \right) dt' \tag{101}$$

Here, Φ_a is given by Eq. (37).

The displacement, strain and stress components are obtained in the same way. For the stress tensor we have, Eq. (25) and (19):

$$\sigma(\rho, z, t) = \int_0^t q'(t') \frac{F_0}{4a(t-t')} \sigma_a \left(\frac{\rho}{\sqrt{4a(t-t')}}, \frac{z}{\sqrt{4a(t-t')}} \right) dt' \tag{102}$$

The components of $\sigma_a(\rho', z')$ are given by Eqs. (57). Alternatively, we can use the explicit expressions in Eqs. (91). The stress is taken for the time $t - t'$, multiplied by $q'(t')$, and integrated in t'. The complete expression for σ_{zz}, for example, becomes from Eq. (91):

$$\sigma_{zz}(\rho, z, t) = \int_0^t q'(t')\, F_0 \left\{ \frac{z}{r^3} \left[\operatorname{erf}\left(\frac{r}{\sqrt{4a(t-t')}} \right) - \frac{2}{\sqrt{\pi}} \frac{r}{\sqrt{4a(t-t')}} e^{-r^2/(4a(t-t'))} \right] \right.$$
$$\left. - \frac{2}{4a(t-t')} e^{-\rho^2/(4a(t-t'))} \operatorname{erf}\left(\frac{z}{\sqrt{4a(t-t')}} \right) \right\} dt' \tag{103}$$

15 Summary of main formulas

The temperature field from the instantaneous, infinite, antisymmetric line heat source, Fig. 1C, is given by Eq. (12). The displacement field with a radial and an axial component is given by Eq. (90). The four non-zero components of the stress field are given by Eqs. (91). The scale factors Φ_0 and F_0 are defined in Eqs. (27). The dimensionless strain field is given by Eqs. (49).

The solution for a finite line heat source, Fig 1B, is obtained by a straight- forward superposition of two infinite, antisymmetric solutions. See Eqs. (93), (95) and (99). The solution for a time-dependent line heat source is obtained by an integration in time involving the instantaneous solutions. See Eqs. (100-103).

References

Abramowitz M., Stegun I.A. 1979. *Handbook of Mathematical Functions*, Dover Publ., New York.

Boley B.A., Weiner J.H. 1960. *Theory of Thermal Stresses*, Wiley, New York.

Carslaw H.S., Jaeger J.C. 1959. *Conduction of Heat in Solids*, 2nd ed., Oxford University Press, Oxford.

Melan E., Parkus H. 1953. *Wärmespannungen infolge stationären Temperaturfelder*, Springer Verlag, Wien.

Parkus H. 1959. *Instationäre Wärmespannungen*, Springer Verlag, Wien.

SKB. 1980-1994. *Annual Reports. Technical Reports*, Swedish Nuclear Fuel and Waste Management Co, Box 5864, S-102 48 Stockholm, Sweden.

Timoshenko S.P., Goodier J.N. 1970. *Theory of Elasticity*, Int. Student Ed. McGraw-Hill, Tokyo.

Nomenclature

a	thermal diffusivity	(m^2/s)
$c\rho_s$	volumetric heat capacity	(J/m^3K)
e	volume expansion, Eq. (7)	(-)
$\mathbf{e}$	unit vector (in the direction of the index), see Fig 2	(-)
erf	error function, Eq. (13)	(-)
erfc	complementary error function, Eq. (13)	(-)
E	Young's modulus	(Pa)
$E_1(x)$	exponential integral, Eq. (108)	(-)
F_0	scale factor for stress, Eqs. (27) and (25)	(N)
H	length of line heat source	(m)
H'	dimensionless half length of line heat source, Eq. (96)	(-)
q_0	heat release per unit length at $t = 0$	(J/m)
$q'(t)$	time dependence of heat release	(-)
r	$= \sqrt{x^2 + y^2 + z^2}$, radial distance	(m)
t	time	(s)
T	temperature	(K)
u	displacement in ρ-direction	(m)
$\mathbf{u}$	displacement vector	(m)
w	displacement in z-direction	(m)
x, y, z	Cartesian coordinates	(m)
z'	$= z/\sqrt{4at}$, dimensionless z-coordinate	(-)
α	coefficient of linear thermal expansion	(1/K)
γ	= 0.5772.., Euler's constant	(-)
ε	strain tensor	(-)
θ	angle to z-axis in spherical coordinates	(-)
ν	Poisson's ratio	(-)
ρ	$= \sqrt{x^2 + y^2}$, distance to z-axis	(m)
ρ'	$= \rho/\sqrt{4at}$, dimensionless distance to z-axis	(-)
σ	stress tensor	(Pa)
σ^a	dimensionless stress tensor for the antisymmetric heat source	(-)
σ'	dimensionless stress tensor for the finite line heat source	(-)
φ	angular coordinate in cylindrical coordinate system	(-)
Φ	displacement potential	(m^2)
Φ_0	scale factor for displacement potential, Eq. (27)	(m^2)

A prime indicates that the quantity is dimensionless. The index a in T_a, Φ_a, $\mathbf{u}_a$, σ_a, $\sigma^a_{\rho\rho}$, etc. refers to the case of an infinite antisymmetric line heat source. These quantities are dimensionless, and they depend only on the dimensionless coordinates ρ' and z'.

Figures 3-16

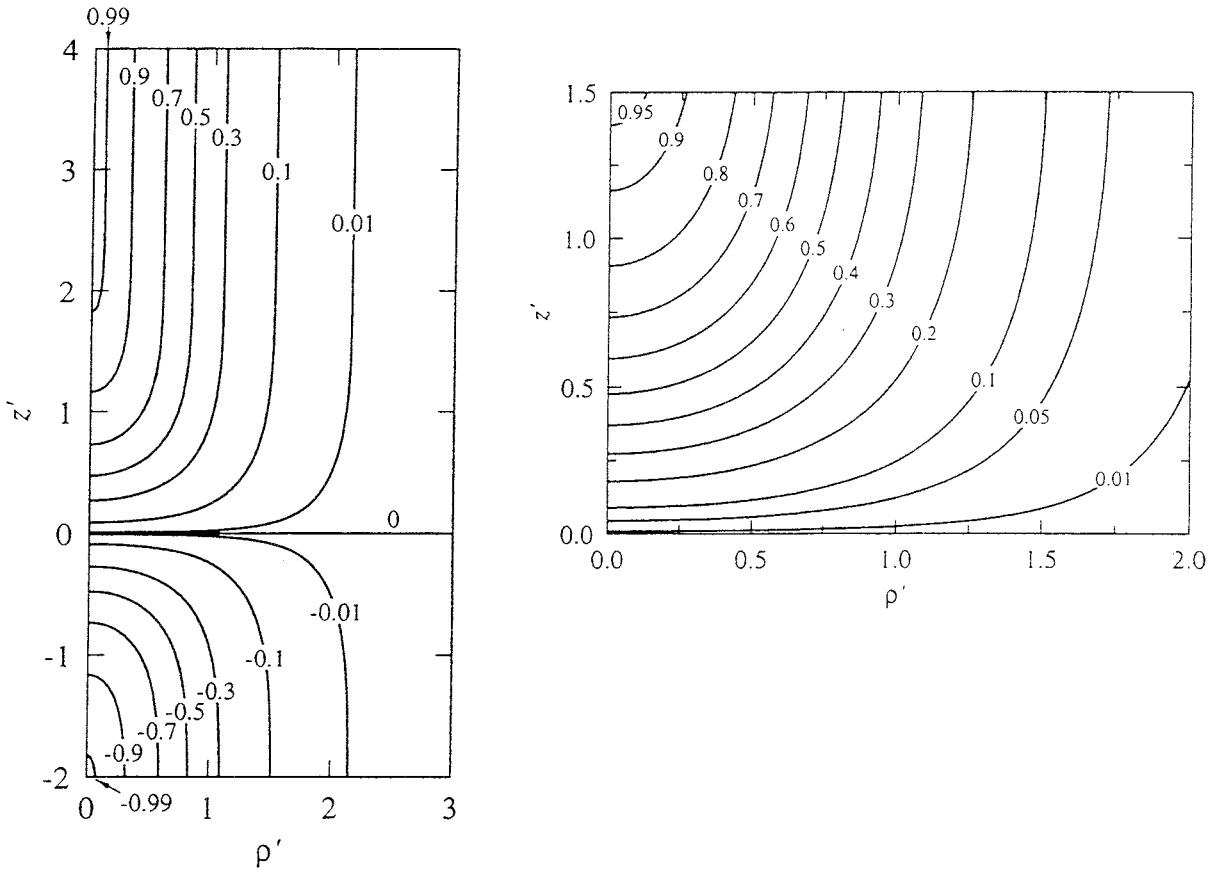

Figure 3: Dimensionless temperature field $T_a(\rho', z')$, Eq. (15), due to the instantaneous, antisymmetric, infinite line heat source along the z'-axis.

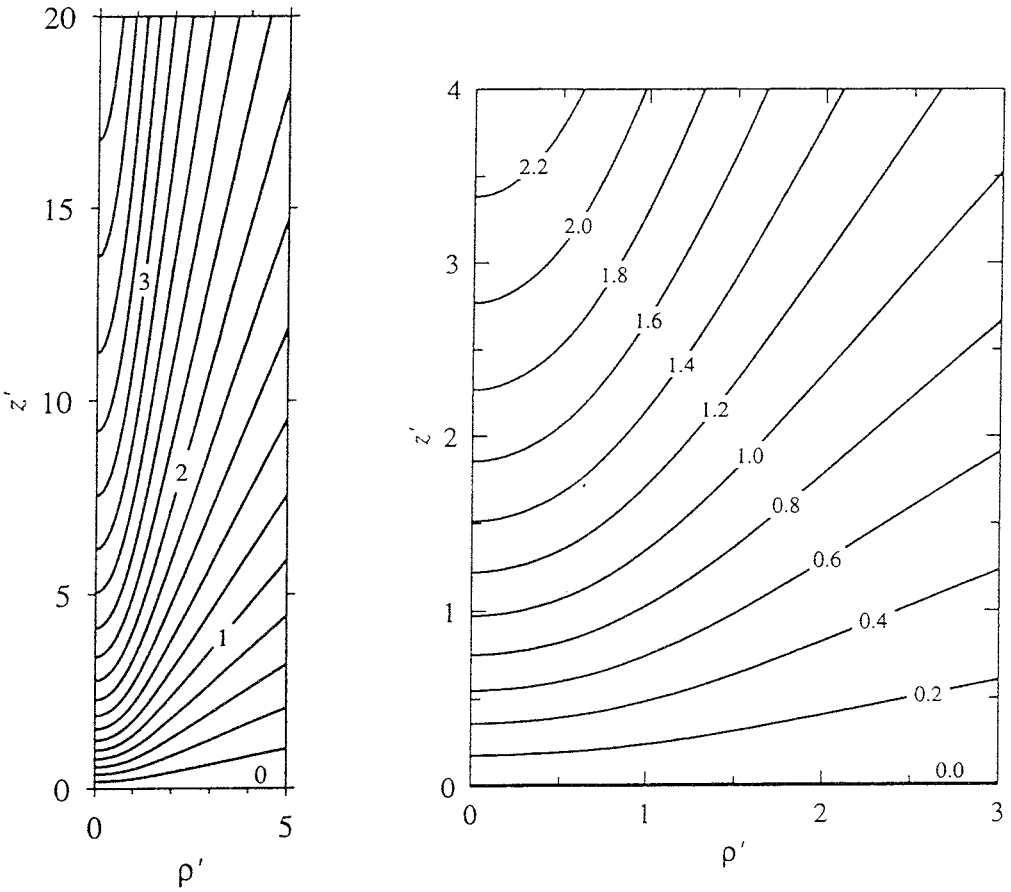

Figure 4: Dimensionless displacement potential $-\Phi_a(\rho', z')$ for the antisymmetric infinite line heat source, Eq. (37).

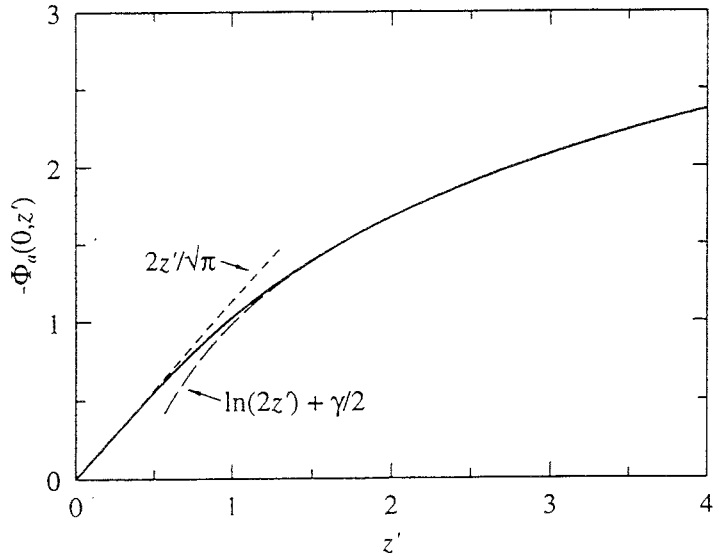

Figure 5: Values of $-\Phi_a$ along the z'-axis.

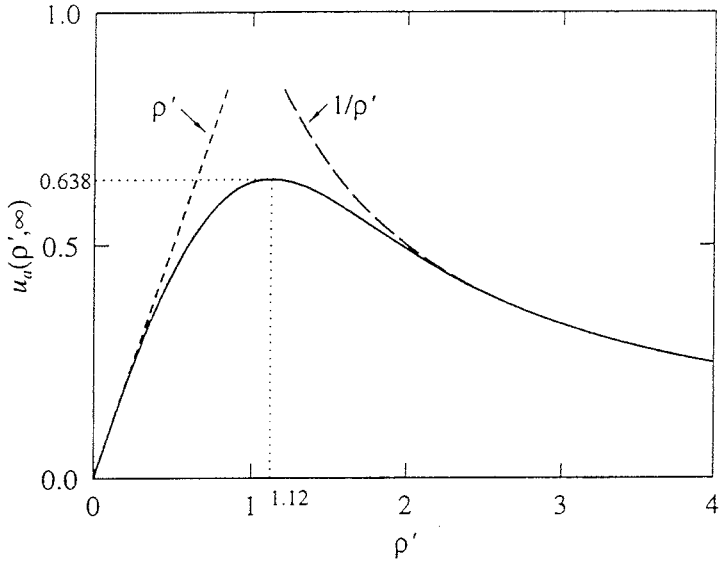

Figure 6: Radial displacement $u_a(\rho', \infty)$ for large z', Eq. (45).

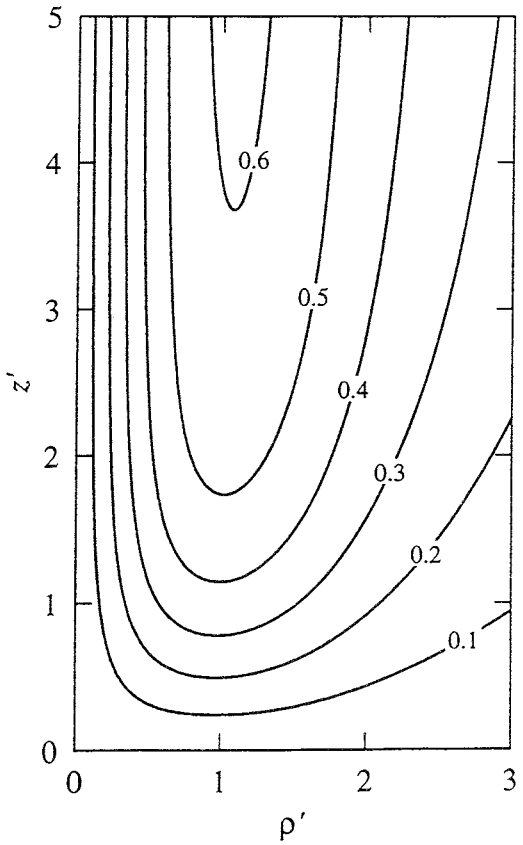

Figure 7: Displacement component $u_a(\rho', z')$ in the ρ-direction, Eq. (40).

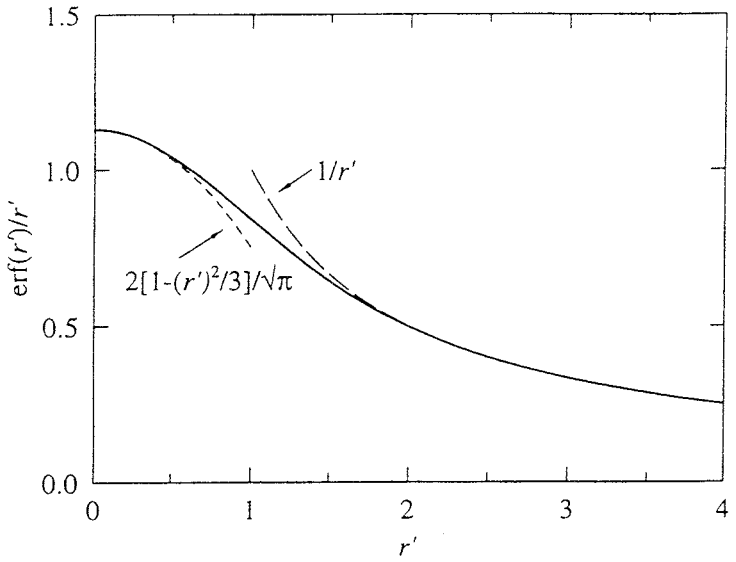

Figure 8: The function $\mathrm{erf}(r')/r'$ which gives w_a, Eq. (41).

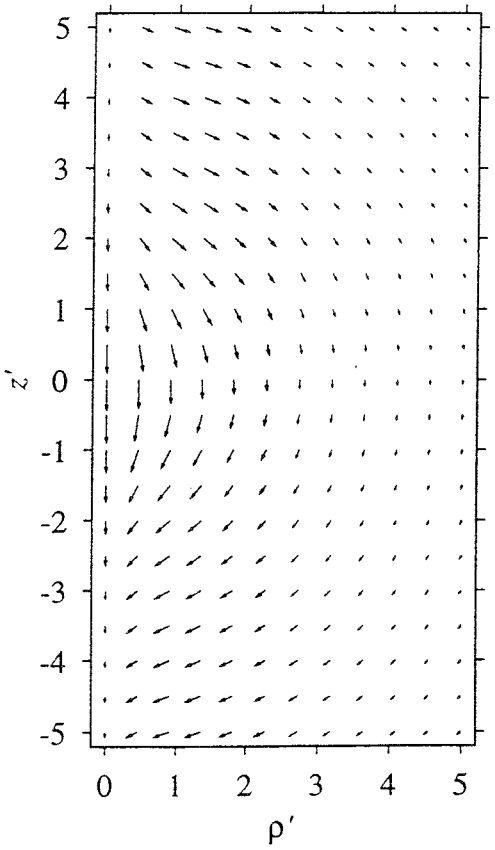

Figure 9: Dimensionless displacement field $\mathbf{u}_a(\rho', z')$, Eqs.(40-41). The largest vector with the magnitude 1.13 occurs at $\rho' = 0$, $z' = 0$.

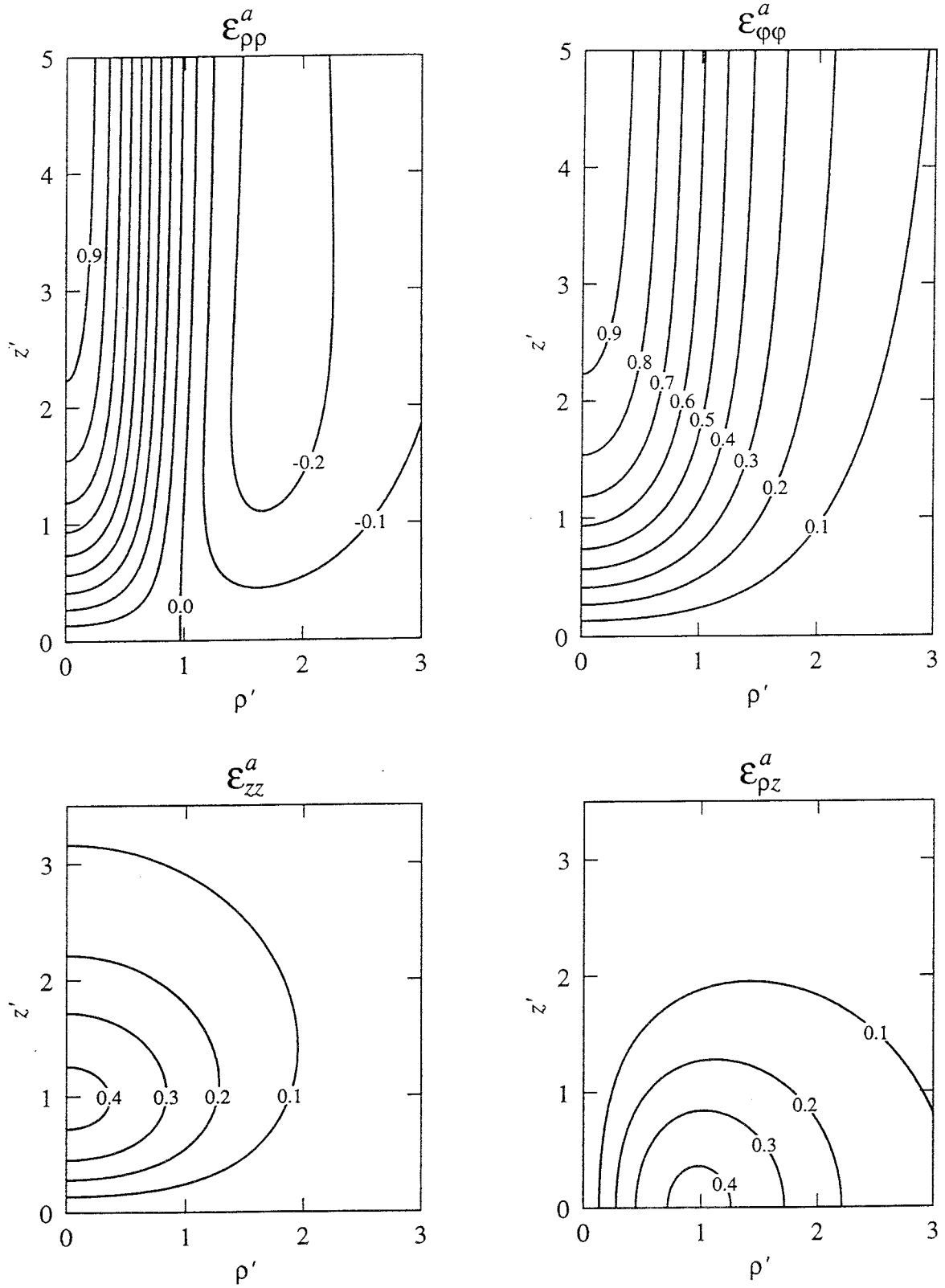

Figure 10: The strain field components $\varepsilon^a_{\rho\rho}$, $\varepsilon^a_{\varphi\varphi}$, ε^a_{zz} and $\varepsilon^a_{\rho z}$, Eqs. (49).

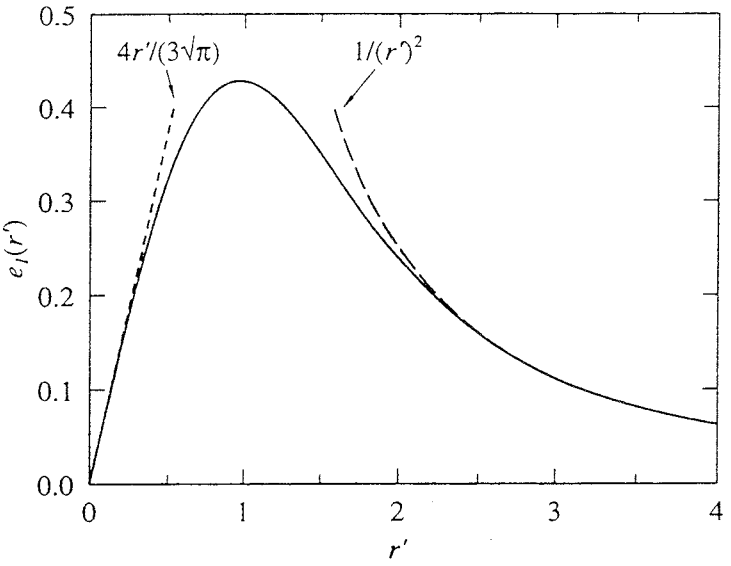

Figure 11: The function $e_1(r')$, Eq. (51).

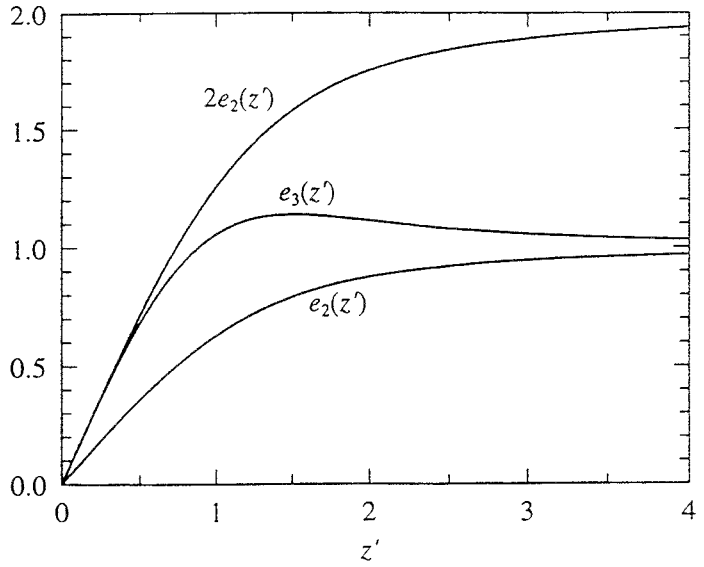

Figure 12: The functions $2e_2(z')$, $e_2(z')$, Eq. (53), and $e_3(z)$, Eq. (60). They give the stress behavior on the z'-axis, Eqs. (63).

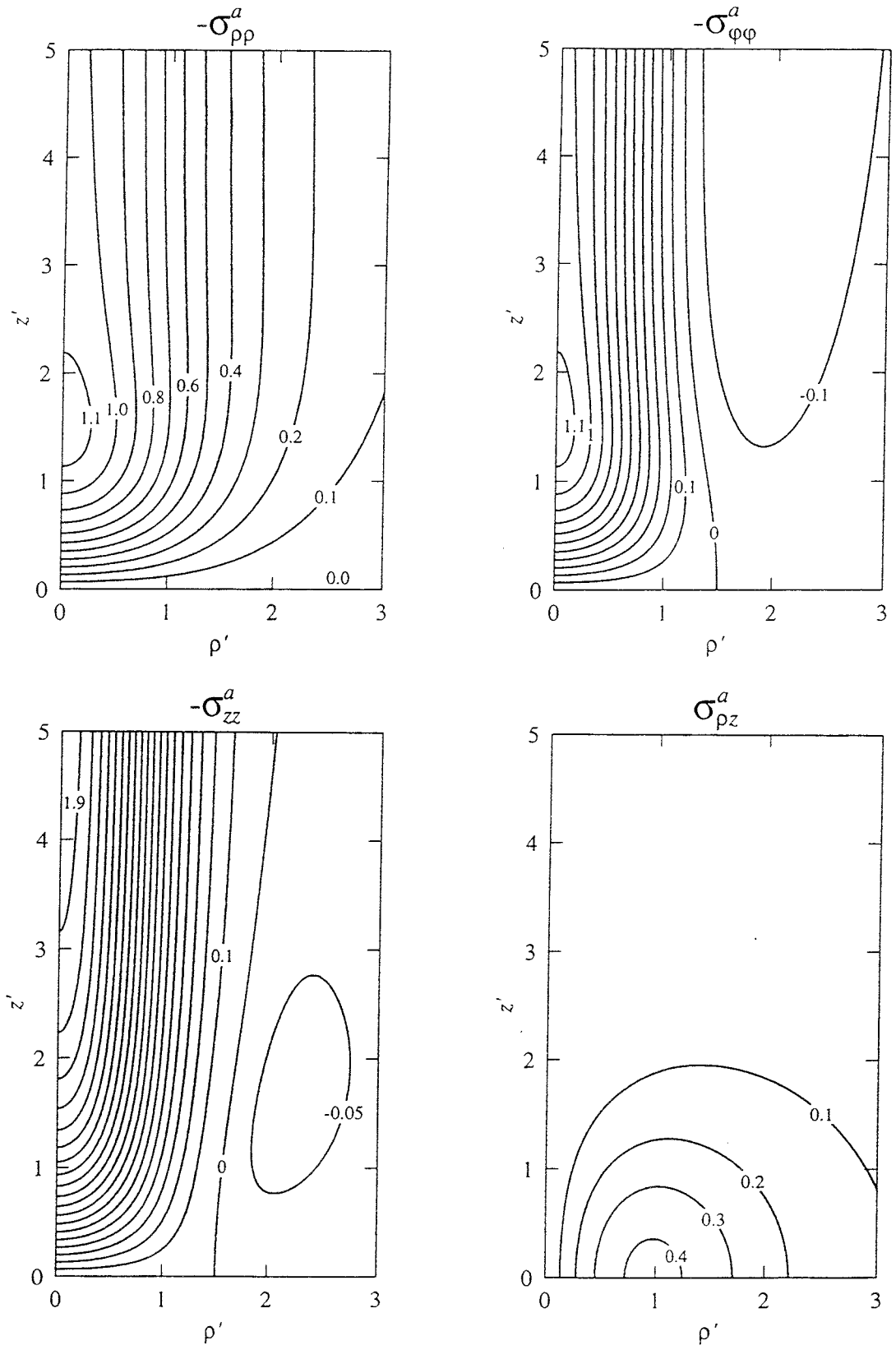

Figure 13: The stress field components $\sigma^a_{\rho\rho}$, $\sigma^a_{\varphi\varphi}$, σ^a_{zz} and $\sigma^a_{\rho z}$, Eqs. (57).

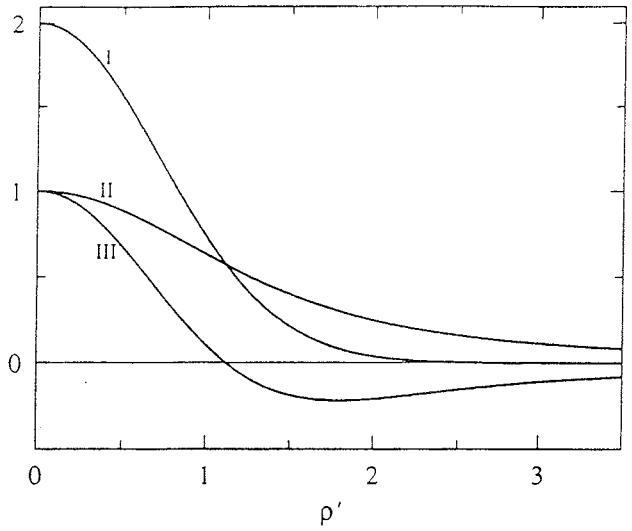

Figure 14: Stress components for $z' = \infty$. I: $-\sigma^a_{zz}(\rho', \infty)$, II: $-\sigma^a_{\rho\rho}(\rho', \infty)$, III: $-\sigma^a_{\varphi\varphi}(\rho', \infty)$, Eqs. (64).

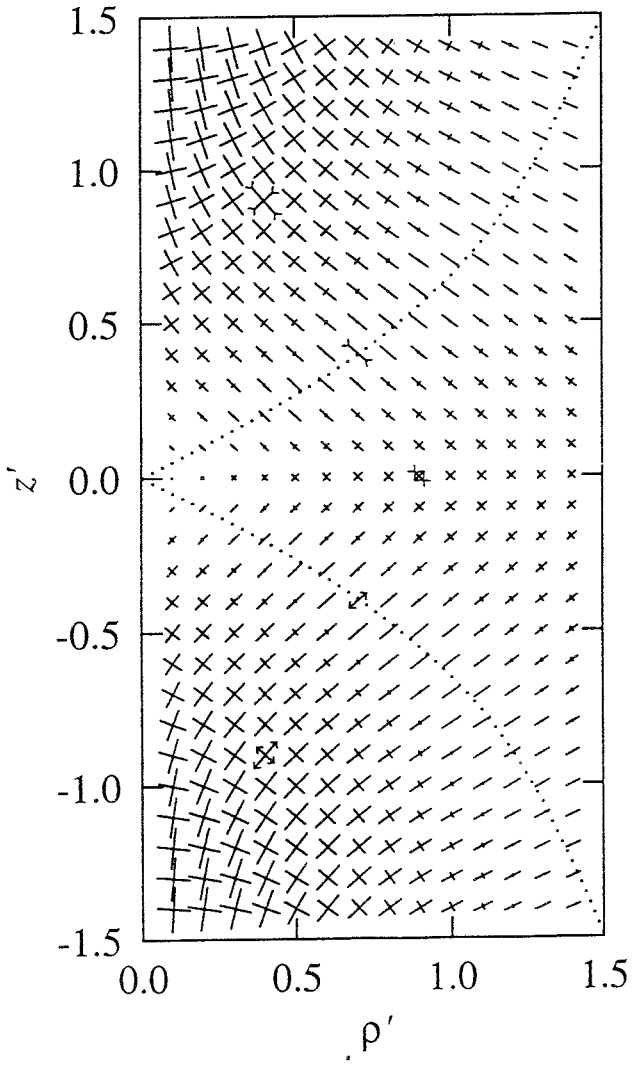

Figure 15: Principal stresses in the (ρ', z')-plane. There is compression in both directions in the top area. On the dotted lines, one of the principal stresses changes sign.

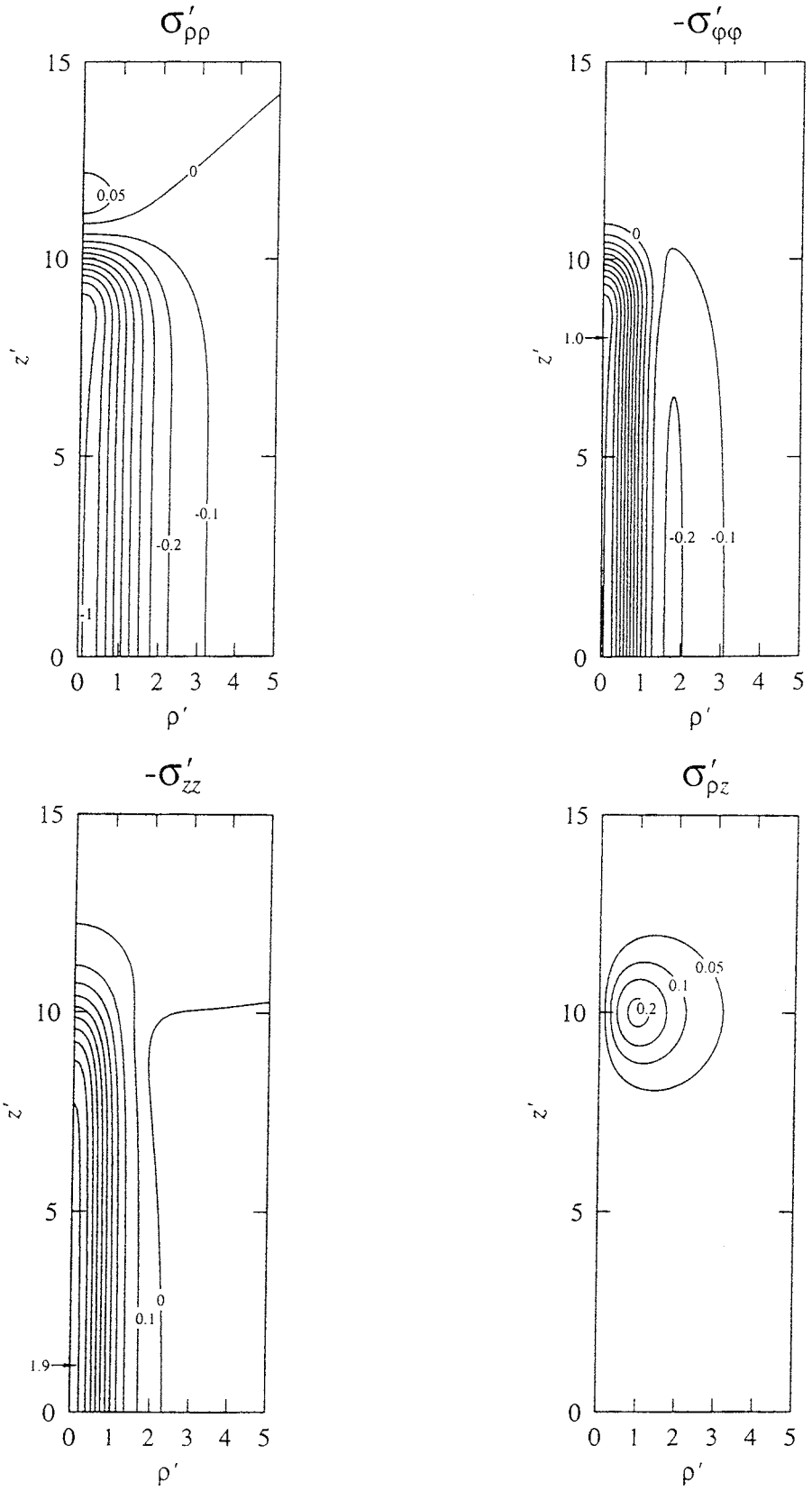

Figure 16: Dimensionless stress field components of the finite line source for $H' = 10$, Eqs. (97) and (57).

Appendix 1. Behavior for large radius

We are interested in the behavior of Φ_a for large r', and in particular for large z' and moderate ρ' near the z'-axis where the line heat source lies.

The integral in Eq. (37) may be rewritten to the following form:

$$\Phi_a(\rho', z') = -\ln\left(\frac{r'+z'}{\rho'}\right) + \int_0^{\cot(\theta)} \frac{\operatorname{erfc}\left(r'\sin(\theta)\sqrt{1+v^2}\right)}{\sqrt{1+v^2}}\, dv \tag{104}$$

Here, erf(..) has been replaced by $1 - \operatorname{erfc}(..)$ in Eq. (37). The logarithm is obtained by integration of $1/\sqrt{(\rho')^2 + s^2}$. Finally, s is substituted by $\rho' v$, $\rho' = r'\sin\theta$, in the remaining integral. The behavior for large r' and fixed θ is readily obtained from Eq. (104). The complementary error function $\operatorname{erfc}(r')$ tends strongly to zero for large r'. So we have:

$$\Phi_a \simeq -\ln\left(\frac{r'+z'}{\rho'}\right) = \ln\left[\tan\left(\theta/2\right)\right] \qquad \text{for large } r', \quad \theta \neq 0, \pi \tag{105}$$

The values $\theta = 0$ and $\theta = \pi$, i.e. the z'-axis, have to be excluded because of the factor $\sin(\theta)$ in the argument of erfc. It should be noted that ρ' becomes large in the above asymptotic expression. The expression is not valid for large z' and small ρ'.

In order to investigate the asymptotic behavior near the z'-axis, we return to integration in s in the integral of Eq. (104) with the substitution $s = \rho' v$. We integrate from zero to infinity in s and subtract the integral from z' to infinity:

$$\Phi_a(\rho', z') = \operatorname{sign}(z') \left[-\ln\left(\frac{r'+|z'|}{\rho'}\right) + \int_0^{\infty} \frac{\operatorname{erfc}\left(\sqrt{(\rho')^2+s^2}\right)}{\sqrt{(\rho')^2+s^2}}\, ds - \int_{|z'|}^{\infty} \frac{\operatorname{erfc}\left(\sqrt{(\rho')^2+s^2}\right)}{\sqrt{(\rho')^2+s^2}}\, ds \right] \tag{106}$$

The factor $\operatorname{sign}(z')$ accounts for negative z'-values.

The first integral, denoted $I(\rho')$, depends on ρ' only:

$$I(\rho') = \int_0^{\infty} \frac{\operatorname{erfc}\left(\sqrt{(\rho')^2+s^2}\right)}{\sqrt{(\rho')^2+s^2}}\, ds \tag{107}$$

We again make the substitution $s = \rho' v$, $\rho' > 0$. The derivative with respect to ρ' becomes:

$$\frac{dI}{d\rho'} = \int_0^{\infty} \frac{1}{\sqrt{1+v^2}}(-1)\frac{2}{\sqrt{\pi}} e^{-(\rho')^2(1+v^2)} \sqrt{1+v^2}\, dv = -\frac{1}{\rho'} e^{-(\rho')^2} \tag{108}$$

The integral $I(\rho')$ is zero for $\rho' = \infty$ (and infinite for $\rho' = 0$). So we have (using the substitution $s^2 = v$):

$$I(\rho') = \int_{\rho'}^{\infty} \frac{e^{-s^2}}{s} ds = 0.5 E_1\left((\rho')^2\right) \tag{109}$$

Here, $E_1(x)$ is the exponential integral, Abramowitz and Stegun (1970):

$$E_1(x) = \int_x^{\infty} \frac{e^{-s}}{s} ds \tag{110}$$

The last integral in Eq. (106) tends to zero for large ρ' and for large $|z'|$. We have the following general asymptotic expression for large r':

$$\Phi_a(\rho', z') \simeq \text{sign}(z') \left[-\ln(r' + |z'|) + \ln(\rho') + 0.5E_1\left((\rho')^2\right)\right] \quad (r' > 2) \tag{111}$$

For large ρ', the expression is equal to Eq. (105), since $E_1(x)$ behaves as $\exp(-x)/x$ for large x. The error in the approximation is given by last integral in Eq. (106). An estimate of this error is:

$$\int_{|z'|}^{\infty} \frac{\text{erfc}\left(\sqrt{(\rho')^2 + s^2}\right)}{\sqrt{(\rho')^2 + s^2}}\, ds \simeq \frac{1}{\sqrt{\pi}} \int_{|z'|}^{\infty} \frac{e^{-(\rho')^2 - s^2}}{(\rho')^2 + s^2}\, ds \lesssim \frac{e^{-(r')^2}}{(r')^2} \cdot \frac{1}{\sqrt{4 + \pi(z')^2} + \sqrt{\pi}|z'|} \tag{112}$$

This estimate is valid for any z' and ρ'.

Near the line heat source, i.e. for small ρ' (and large $|z'|$), we have:

$$-\ln(r' + |z'|) \simeq -\ln(2|z'|) - \frac{1}{4}\left(\frac{\rho'}{z'}\right)^2 \qquad (\rho' < 0.5,\ |z'| > 2)$$

$$0.5E_1\left((\rho')^2\right) + \ln(\rho') \simeq -\frac{\gamma}{2} + \frac{(\rho')^2}{2} \qquad (\rho' < 0.5) \tag{113}$$

Here, $\gamma = 0.5772\ldots$ is Euler's constant. A series expansion of E_1 is used in the second equation. Equation (111) becomes for small ρ' and large $|z'|$:

$$\Phi_a(\rho', z') \simeq \text{sign}(z') \left[-\ln(2|z'|) - \gamma/2 + \frac{(\rho')^2}{2} - \frac{1}{4}\left(\frac{\rho'}{z'}\right)^2 \right] \qquad (\rho' < 0.5,\ |z'| > 2) \tag{114}$$

In particular, we have for $\rho' = 0$:

$$\Phi_a(0, z') \simeq \text{sign}(z') \left[-\ln(2|z'|) - \gamma/2 \right] \qquad (|z'| > 2) \tag{115}$$

This asymptotic expression is shown in Fig. 6.

The derivatives of the approximate expression for $\Phi_a(\rho', z')$, Eq. (111), give the asymptotic displacement components of Eqs. (78). The asymptotic expressions given in Section 11 follow from Eq. (111).

Appendix 2. Behavior for small radius

The behavior for small r' is also of interest. A series expansion of erf $\left(\sqrt{(\rho')^2 + s^2}\right)$ in Eq. (37) gives:

$$\Phi_a(\rho', z') = -\frac{2}{\sqrt{\pi}} \int_0^{z'} \left[1 - \frac{(\rho')^2 + s^2}{3} + \frac{\left((\rho')^2 + s^2\right)^2}{10} + \ldots \right] ds \tag{116}$$

or

$$\Phi_a(\rho', z') = -\frac{2}{\sqrt{\pi}} \left[z' - \frac{(\rho')^2 z'}{3} - \frac{(z')^3}{9} + \frac{(\rho')^4 z'}{10} + \frac{(\rho')^2 (z')^3}{15} + \frac{(z')^5}{50} - \ldots \right] \qquad (r < 0.5) \tag{117}$$

The first derivatives of $\Phi_a(\rho', z')$ give the displacement components:

$$u_a \simeq \frac{4\rho' z'}{3\sqrt{\pi}}\left(1 - \frac{3(\rho')^2 + (z')^2}{5}\right) \qquad w_a \simeq -\frac{2}{\sqrt{\pi}}\left(1 - \frac{(\rho')^2 + (z')^2}{3}\right) \qquad (r' < 0.5) \tag{118}$$

Second derivatives of $\Phi_a(\rho', z')$ give the strain, Eqs. (29):

$$\varepsilon^a_{\rho\rho} \simeq \frac{4z'}{3\sqrt{\pi}}\left(1 - \frac{9(\rho')^2 + (z')^2}{5}\right) \qquad \varepsilon^a_{\varphi\varphi} \simeq \frac{4z'}{3\sqrt{\pi}}\left(1 - \frac{3(\rho')^2 + (z')^2}{5}\right)$$

$$\varepsilon^a_{zz} \simeq \frac{4z'}{3\sqrt{\pi}}\left(1 - \frac{3(\rho')^2 + 3(z')^2}{5}\right) \qquad \varepsilon^a_{\rho z} \simeq \frac{4\rho'}{3\sqrt{\pi}}\left(1 - \frac{3(\rho')^2 + 3(z')^2}{5}\right) \qquad (r' < 0.5) \tag{119}$$

The temperature T_a becomes:

$$T_a \simeq \frac{2z'}{\sqrt{\pi}}\left(1 - (\rho')^2 - \frac{(z')^2}{3}\right) \tag{120}$$

The stress components become from Eqs. (30):

$$\sigma^a_{\rho\rho} \simeq -\frac{8z'}{3\sqrt{\pi}}\left(1 - \frac{3(\rho')^2 + 2(z')^2}{5}\right) \qquad \sigma^a_{\varphi\varphi} \simeq -\frac{8z'}{3\sqrt{\pi}}\left(1 - \frac{6(\rho')^2 + 2(z')^2}{5}\right)$$

$$\sigma^a_{zz} \simeq -\frac{8z'}{3\sqrt{\pi}}\left(1 - \frac{6(\rho')^2 + (z')^2}{5}\right) \qquad \sigma^a_{\rho z} \simeq \frac{4\rho'}{3\sqrt{\pi}}\left(1 - \frac{3(\rho')^2 + 3(z')^2}{5}\right) \qquad (r' < 0.5) \tag{121}$$

The first-order term of the normal stresses becomes, Eq. (71):

$$\sigma^a_1 \simeq -\frac{8}{3\sqrt{\pi}}\left(z' - \frac{\rho'}{2}\right) \qquad \sigma^a_2 \simeq -\frac{8}{3\sqrt{\pi}}\left(z' + \frac{\rho'}{2}\right) \qquad \sigma^a_3 \simeq -\frac{8}{3\sqrt{\pi}}\, z' \qquad (r' < 0.5) \tag{122}$$

List of SKB reports

Annual Reports

1977-78
TR 121
KBS Technical Reports 1 – 120
Summaries
Stockholm, May 1979

1979
TR 79-28
The KBS Annual Report 1979
KBS Technical Reports 79-01 – 79-27
Summaries
Stockholm, March 1980

1980
TR 80-26
The KBS Annual Report 1980
KBS Technical Reports 80-01 – 80-25
Summaries
Stockholm, March 1981

1981
TR 81-17
The KBS Annual Report 1981
KBS Technical Reports 81-01 – 81-16
Summaries
Stockholm, April 1982

1982
TR 82-28
The KBS Annual Report 1982
KBS Technical Reports 82-01 – 82-27
Summaries
Stockholm, July 1983

1983
TR 83-77
The KBS Annual Report 1983
KBS Technical Reports 83-01 – 83-76
Summaries
Stockholm, June 1984

1984
TR 85-01
Annual Research and Development Report 1984
Including Summaries of Technical Reports Issued during 1984. (Technical Reports 84-01 – 84-19)
Stockholm, June 1985

1985
TR 85-20
Annual Research and Development Report 1985
Including Summaries of Technical Reports Issued during 1985. (Technical Reports 85-01 – 85-19)
Stockholm, May 1986

1986
TR 86-31
SKB Annual Report 1986
Including Summaries of Technical Reports Issued during 1986
Stockholm, May 1987

1987
TR 87-33
SKB Annual Report 1987
Including Summaries of Technical Reports Issued during 1987
Stockholm, May 1988

1988
TR 88-32
SKB Annual Report 1988
Including Summaries of Technical Reports Issued during 1988
Stockholm, May 1989

1989
TR 89-40
SKB Annual Report 1989
Including Summaries of Technical Reports Issued during 1989
Stockholm, May 1990

1990
TR 90-46
SKB Annual Report 1990
Including Summaries of Technical Reports Issued during 1990
Stockholm, May 1991

1991
TR 91-64
SKB Annual Report 1991
Including Summaries of Technical Reports Issued during 1991
Stockholm, April 1992

1992
TR 92-46
SKB Annual Report 1992
Including Summaries of Technical Reports Issued during 1992
Stockholm, May 1993

1993
TR 93-34
SKB Annual Report 1993
Including Summaries of Technical Reports Issued during 1993
Stockholm, May 1994

1994

TR 94-33

SKB Annual Report 1994

Including Summaries of Technical Reports Issued during 1994.
Stockholm, May 1995

1995

TR 95-37

SKB Annual Report 1995

Including Summaries of Technical Reports Issued during 1995.
Stockholm, May 1996

List of SKB Technical Reports 1996

TR 96-01

Bacteria, colloids and organic carbon in groundwater at the Bangombé site in the Oklo area

Karsten Pedersen (editor)
Department of General and Marine Microbiology, The Lundberg Institute, Göteborg University, Göteborg, Sweden
February 1996

TR 96-02

Microbial analysis of the buffer/container experiment at AECL´s Underground Research Laboratory

S Stroes-Gascoyne[1], K Pedersen[2], S Daumas[3], C J Hamon[1], S A Haveman[1], T L Delaney[1], S Ekendahl[2], N Jahromi[2], J Arlinger[2], L Hallbeck[2], K Dekeyser[3]

[1] AECL, Whiteshell Laboratories, Pinawa, Manitoba, Canada
[2] University of Göteborg, Department of General and Marine Microbiology, Göteborg, Sweden
[3] Guigues Recherche Appliquée en Microbiologie (GRAM), Aix-en-Provence, France
1996

TR 96-03

Reduction of Tc (VII) and Np (V) in solution by ferrous iron. A laboratory study of homogeneous and heterogeneous redox processes

Daqing Cui, Trygve E Eriksen
Department of Chemistry, Nuclear Chemistry, Royal Institute of Technology, Stockholm, Sweden
March 1996

TR 96-04

Revisiting Poços de Caldas. Application of the co-precipitation approach to establish realistic solubility limits for performance assessment

Jordi Bruno, Lara Duro, Salvador Jordana, Esther Cera
QuantiSci, Barcelona, Spain
February 1996

TR 96-05

SR 95

Template for safety reports with descriptive example
SKB
December 1995

TR 96-06

Äspö Hard Rock Laboratory Annual Report 1995

SKB
April 1996

TR 96-07

Criticality in a high level waste repository. A review of some important factors and an assessment of the lessons that can be learned from the Oklo reactors

Virginia M Oversby
VMO Konsult
June 1996

TR 96-08

A reappraisal of some Cigar Lake issues of importance to performance assessment

John Smellie[1], Fred Karlsson[2]

[1] Conterra AB
[2] SKB
July 1996

TR 96-09

The long-term stability of cement. Leaching tests

Ingemar Engkvist, Yngve Albinsson, Wanda Johansson Engkvist
Chalmers University of Technology, Göteborg, Sweden
June 1996

TR 96-10

Lake-tilting investigations in southern Sweden

Tore Påsse
Sveriges geologiska undersökning, Göteborg, Sweden
April 1996